CHAPTER 11

Reliability and Life Prediction of Ceramic Composite Structures at Elevated Temperatures

S. F. Duffy and J. P. Gyekenyesi

11.1 Introduction

Engineered materials are poised to supplant conventional metal alloys in numerous applications. A variety of engineered materials have been proposed that increase either strength, fracture toughness, or both. For the most part, successful engineered materials have exploited transformation toughening caused by constituents undergoing a stress-induced martensitic transformation, or have embedded long fibers and particulate reinforcements in a matrix material to enhance the fracture or deformation behavior in a particular direction. It is anticipated that the availability of engineered materials in large quantities will herald the advent of new products that have been conceptualized, but are awaiting the right material with an optimum set of properties. Crucial material properties may vary for many industrial and aerospace applications; however, most applications will require high specific stiffness, strength, and toughness (which must be maintained at elevated temperatures in aggressive environments), and low density. A breakthrough material will possess the right property mix at a price that allows components to be fabricated economically.

The engineered material systems focused on here are composites with ceramic matrices reinforced with ceramic fibers. Monolithic ceramics exhibit useful properties such as retention of strength at high temperatures, chemical inertness, and low density. However, the use of monolithic ceramics has been limited by their inherent brittleness, susceptibility to damage from thermal shock, and a large variation in strength which is reflected in diminished component reliabilities. Adding a second ceramic phase with an optimized interface to a brittle matrix improves fracture toughness, decreases the sensitivity to microscopic flaws and, depending on the constituents and

direction, may also increase strength. The presence of fibers in the vicinity of a critical defect modifies fracture behavior by increasing the required crack driving force through several mechanisms. These mechanisms include crack pinning, fiber bridging, fiber debonding, and fiber pull-out. This increase in fracture toughness allows for graceful rather than catastrophic failure.

Ceramic composite material systems have been produced using a variety of reinforcing schemes. These include whiskers, chopped fibers, particulates, long fibers, and woven fibers as reinforcements. In some instances, two types of reinforcements have been commingled to produce a hybrid ceramic matrix composite (CMC). These emerging composite materials can compete with metals in many demanding applications. Prototypes fabricated from the materials just mentioned have already demonstrated functional capabilities at temperatures approaching 1400°C, which is well beyond the operational limit of most metallic material systems, including composites manufactured from superalloys. Indeed the focus of this text and the issues concentrated on in this chapter primarily relate to the use of ceramic matrix composites at elevated service temperatures.

The authors anticipate that the majority of near-term high temperature applications of components fabricated from ceramic matrix composites will be found in the power generation and the aerospace industries. The use of gas turbines is being advocated in meeting peak service demands in the electric power industry. In addition, progress in utilizing aero-derivative gas turbines has supported cogeneration technologies. Cogeneration (combined cycle) power plants are able to utilize the exhaust gases from gas turbines to generate steam. Due to low costs, improved efficiency ratings, and plentiful supply of natural gas, cogeneration power plants will play a significant role in future electric power generation. Use of CMC material systems in power generation applications (as well as marine propulsion systems) has given rise to expectations of increased fuel efficiency, multifuel capability, and meeting stringent emission standards.

There are many potential aerospace applications of CMC material systems currently under consideration. Examples include propulsion subsystems in High Speed Civil Transport (HSCT). In this program, ceramic composites are being proposed for use as segmented combustor liners and exhaust nozzles. CMC materials are also under consideration in the fabrication of components for advanced gas-turbine engines, including small missile turbine rotors. Ceramic matrix composites offer a significant potential for raising the thrust-to-weight ratio of gas-turbine engines by tailoring directions of high specific reliability. Improvements in fuel efficiency are anticipated due to increased engine temperatures and pressures, which, in turn, generate more power and thrust. The anticipated goals again include developing multifuel capability, and reducing NO_x (oxides of nitrogen) emissions. For these reasons, programs such as HSCT and the National Aero-Space Plane (NASP) advocate the use of CMC materials in critical hot sections of advanced propulsion systems.

The use of ceramic matrix composites is not limited to the two fields cited above. Other potential industrial applications include various components of automotive engines, heat exchangers, waste incinerators, and membrane filtration systems. These include applications with ambient and elevated service temperatures. CMC materials should be considered in any application where toughness and wear resistance are key design factors, or where components are subjected to high service temperature in corrosive environments. In the near term, aqueous waste processing and diesel engine exhaust filters are examples of separation and purification processes that represent potential markets for this material system. In addition, components fabricated from CMC materials are currently employed in heat exchanger design. Examples include recuperators, bayonet and plate-fin heat exchangers. Wherever stringent performance criteria are specified in operating environments that challenge the limits of metal-based material systems, CMC materials will provide viable alternatives.

Yet the impact of CMC materials will be felt only as engineers become comfortable designing components fabricated from these materials. As noted in the following sections, a number of aspects relating to the mechanical behavior of ceramic matrix composites necessitates reconsidering traditional design methods. To meet this challenge, this chapter can be used as an aid for those individuals willing to pursue the probabilistic methods that address the mechanical response of ceramic matrix composites. Many references are provided to enable the reader to pursue a topic in greater detail than is allowed for here. It was noted earlier that the focus of this text is the use of ceramic matrix composites in applications with elevated service temperatures. To this end, the authors have highlighted methods to ascertain the structural reliability of components subject to quasi-static load conditions. Each method focuses on a particular composite microstructure. In addition, since elevated service temperatures usually involve time-dependent effects, a section dealing with reliability degradation as a function of load history has been included. However, this field of research is not as mature as the other issues covered here, and it is treated in a preliminary fashion. The authors believe that as these new design concepts are embraced, fabricating components from ceramic matrix composites will take place in large volumes. As a result, manufacturing economies of scale will quickly bring fabrication costs in line with the more conventional material systems.

In addressing issues relating to component failure, the reader will note a recurring theme throughout this chapter. Even though component failure is controlled by a sequence of many microfailure events, failure of ceramic composites will be modeled using macrovariables. The sheer number and order of microfailure events will preclude the design engineer from predicting analytically the sequence of events leading to component failure (in whatever manner this macro-level event is defined). This does not imply that the engineer can design components fabricated from CMC material systems without a working knowledge of the physics of failure taking place within the microstructure of a ceramic composite. However, it is the authors' viewpoint

that failure at the component level can best be described with phenomenological failure models using macrovariables. At this point micromechanics is ill-suited for component failure analyses, yet it can be utilized quite effectively in predicting global stiffness properties. Although global stiffness properties are extremely important when designing components fabricated from composite materials, with the exception of woven ceramic composites, this subject is not discussed here. Otherwise, the reader is directed to the wealth of literature in this field (e.g., Rosen[1] and McCullough[2]). In the case of woven ceramic composites the authors provide a focused literature survey regarding the prediction of stiffness properties for this emerging material system.

11.2 Whisker-Toughened Ceramics

11.2.1 Introduction

The reason behind adding a second ceramic phase is that through proper tailoring of the composite microstructure one can dramatically improve the mechanical properties (fracture toughness and creep resistance) of monolithic ceramics. For ceramic matrix composites this effort began with attempts to uniformly disperse whiskers and particle reinforcements with tailored interfaces throughout a ceramic matrix. Conceptually, one hopes to perturb the stress field in the vicinity of the tip of a critical matrix crack with the inclusion of a second phase. This should cause a reduction in the stress intensity. Lange[3] originally proposed a method to compute the stress necessary to propagate a crack front that bows between two obstacles, and developed a modified Griffith equation where the increase in fracture surface energy is directly related to a line tension effect. The approach assumes that the whiskers have a higher fracture toughness than the matrix, and that the crack front penetrates the matrix material in a nonlinear fashion (i.e., "bows out"). The postulated behavior is analogous to the motion of dislocations through a precipitate-hardened material. Evans[4] and Green[5] have suggested modifications to this model that account for whisker morphologies. Toughening by crack deflection arises from the crack front tilting and/or twisting as it encounters the second phase. This produces noncoplanar crack extension and a decreased stress intensity at the crack tip. The direction taken by the crack front after deflection is controlled by whisker morphology and the residual stress field (e.g., tensile or compressive) arising from high temperature processing and subsequent cooling. A fracture mechanics model for crack deflection has been proposed by Faber and Evans[6] that accounts for mixed-mode behavior. Angelini and Becher[7] have presented evidence from electron microscopy observations that indicates whiskers may bridge the crack as it propagates. Based on these data, Becher and co-workers[8] developed a model to predict the increase in fracture toughness due to the closure stresses imposed on the crack by the bridging whiskers. Finally, Wetherhold[9] developed a model based on probabilistic

principles that enables the computation of increased energy absorption during fracture due to whisker pull-out. However, compared to continuous fiber-reinforced ceramics (discussed in Section 11.3), whisker pull-out is limited due to the short lengths of the whiskers (typically less than 100 μm).

The primary intent of the models mentioned above is to consider the composite as a structure and develop predictive methods to optimize the microstructure. Ultimately, one would then make use of these concepts to similarly refine the design of structural components. Whenever practical, elegant design methods incorporate the relevant physics of failure into the analysis of the macroscopic response of a component. However, at this point difficulties arise that prevent taking this approach in the analysis of components manufactured from whisker-toughened ceramics. First, the crack mitigation processes strongly interact, and it is difficult to experimentally detect or analytically predict the sequence of mechanisms leading to failure (e.g., crack deflection, then whisker pull-out, then crack bridging, etc.). Furthermore, with the exception of the model by Faber and Evans,[6] the methods mentioned previously only consider Mode I failure. This precludes conducting a structural analysis on a component subject to multiaxial states of stress that vary from point to point in the component. Finally, these initial analytical techniques have focused primarily on predicting behavior using deterministic approaches. Even though improved processing techniques have resulted in the reduction of inhomogeneities, uniform whisker distributions, and dense matrices, failure remains a stochastic process for discrete particle-toughened materials.

An alternate approach that conveniently sidesteps the aforementioned obstacles is to compute reliability in terms of macrovariables using phenomenological criteria. Focusing a design approach at the macroscopic level represents a minor philosophical drawback, for it excludes any consideration of the microstructural events that involve interactions between individual whiskers and the matrix. The phenomenological point of view implies that the material element under consideration is small enough to be homogeneous in stress and temperature, yet large enough to contain a sufficient number of whiskers such that the element is a statistically homogeneous continuum. Obviously these conditions cannot always be met for they depend on characteristic component dimensions, the severity of gradients within the component, and the geometry of the microstructure. When these conditions are satisfied, one can systematically formulate multiaxial reliability models under the assumption that the material is homogeneous, with stochastic properties and behavior that can be deduced from well-chosen phenomenological experiments. From a historical perspective, phenomenological approaches are usually (but not always) supplanted by techniques that accurately reflect the physics of the microstructure. Precedence for this can be found in modeling monolithic ceramics where the detailed concepts of Batdorf and Crose[10] have, for the most part, superseded phenomenological approaches such as the reliability model based on the principle of independent action (PIA: see Shih[11]).

11.2.2 Noninteractive Reliability Models

Duffy *et al.*[12] presented the details of using phenomenological approaches in designing whisker-toughened ceramic components. Depending on fabrication, a whisker-toughened composite may have an isotropic, transversely isotropic, or orthotropic material symmetry. One can postulate that a model based on the principle of independent action would be an appropriate first approximation phenomenological theory for isotropic whisker composites. However, an interactive reliability model presented in the next section more accurately reflects anticipated phenomenological behavior such as reduced scatter in compression, and sensitivity to the hydrostatic component of the stress state. Duffy and Arnold[13] presented a noninteractive phenomenological model for whisker-toughened composites with a transversely isotropic material symmetry often encountered in hot-pressed and injection-molded whisker-toughened ceramics. In their discussion, reliability is governed by weakest link theory. The existence of a failure function per unit volume was assumed, where the unit volume was considered as an individual link. The failures of the individual links are considered as statistical events, which are assumed to be independent. Defining f as the failure of an individual link, then

$$f = \psi \Delta V \tag{1}$$

where V denotes volume and ψ is the failure function. Taking r as the reliability of an individual link, then

$$r = 1 - \psi \Delta V \tag{2}$$

The reliability of the continuum, denoted as R, is

$$\begin{aligned} R &= \lim_{N \to \infty} \left[\prod_{\xi=1}^{N} r_\xi \right] \\ &= \lim_{N \to \infty} \left[\prod_{\xi=1}^{N} [1 - \psi(x_i) \Delta V]_\xi \right] \end{aligned} \tag{3}$$

Here $\psi(x_i)$ is the failure function per unit volume at position x_i within the continuum, and N is the number of links in the continuum. Unless noted otherwise, roman letter subscripts denote tensor indices with an implied range from 1 to 3. Greek letter subscripts are associated with products or summations with ranges that are explicit in each expression. Adopting an argument used by Cassenti,[14] the reliability of the continuum is given by the following expression

$$R = \exp\left[- \int_V \psi dV \right] \tag{4}$$

As was noted earlier, a reliability model based on the principle of independent action would be a candidate for a first approximation macroscopic

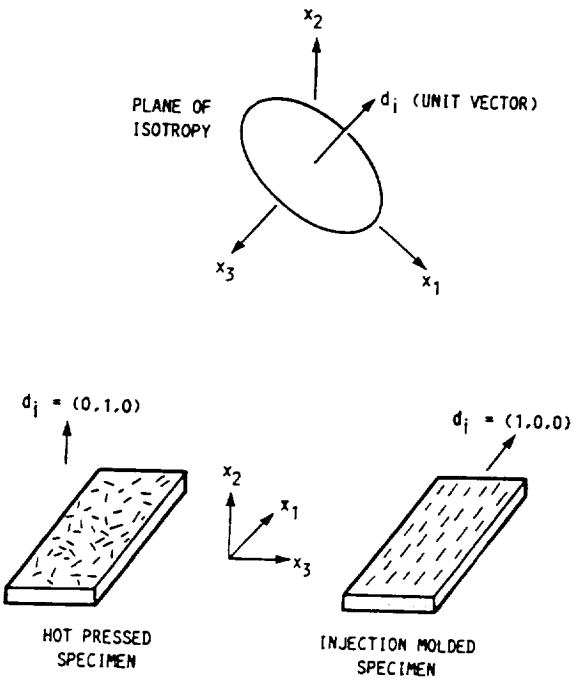

Fig. 11.1 Examples of transversely isotropic whisker-reinforced ceramic composites.

theory for isotropic whisker composites. In this instance, the failure function ψ would depend only upon stress, or the principal invariants of stress, i.e.,

$$\psi = \psi(\sigma_{ij})$$
$$= \psi(\sigma_1, \sigma_2, \sigma_3) \tag{5}$$

where σ_{ij} is the Cauchy stress tensor and σ_1, σ_2 and σ_3 are the associated principal stresses. However, a more comprehensive reliability model for isotropic whisker-toughened ceramics is pressented in the next section. For transversely isotropic whisker composites, the failure function must also reflect material symmetry. This requires

$$\psi = \psi(\sigma_{ij}, d_i) \tag{6}$$

where d_i is a unit vector that identifies a local material orientation. This orientation, depicted in Fig. 11.1, is defined as the normal to the plane of isotropy.

The sense of d_i is immaterial, thus its influence is taken into account through the product $d_i d_j$, i.e.

$$\psi = \psi(\sigma_{ij}, d_i d_j) \tag{7}$$

Note that $d_i d_j$ is a symmetric second-order tensor whose trace satisfies the identity

$$d_i d_i = 1 \tag{8}$$

Furthermore, the stress and local preferred direction may vary from point to point in the continuum. Thus Eqn. (7) implies that the stress field and unit vector field, i.e. $\sigma_{ij}(x_k)$ and $d_i(x_k)$, must be specified to define ψ. Current state of the art in designing structural components uses finite element methods to characterize the stress field. The reader will see shortly that this is conveniently utilized in analyzing component reliability.

Since ψ is a scalar valued function, it must remain form invariant under arbitrary proper orthogonal transformations. Work by Reiner,[15] Rivlin and Smith,[16] Spencer,[17] and others, demonstrates that through the application of the Cayley–Hamilton theorem and elementary properties of tensors, a finite set of invariants known as an integrity basis can be developed. Form invariance of ψ is ensured if dependence is taken on invariants that constitute the integrity basis, or any subset thereof. Adapting the above-mentioned work to ψ results in an integrity basis composed of ten tensor products. Following arguments similar to Spencer,[18] several of these tensor products are equal and others are trivial identities such that the final integrity basis for ψ contains only the invariants

$$I_1 = \sigma_{ii} \tag{9}$$

$$I_2 = \sigma_{ij}\sigma_{ji} \tag{10}$$

$$I_3 = \sigma_{ij}\sigma_{jk}\sigma_{ki} \tag{11}$$

$$I_4 = d_i d_j \sigma_{ji} \tag{12}$$

and

$$I_5 = d_i d_j \sigma_{jk}\sigma_{ki} \tag{13}$$

A slightly different set of invariants that corresponds to components of the stress tensor oriented to the material direction can be constructed from the above integrity basis. This new set of invariants includes

$$\hat{I}_1 = I_4 \tag{14}$$

$$\hat{I}_2 = [I_5 - (I_4)^2]^{1/2} \tag{15}$$

$$\hat{I}_3 = (\tfrac{1}{2})(I_1 - I_4) + [(\tfrac{1}{2})I_2 - I_5 + \tfrac{1}{4}(I_4)^2 - \tfrac{1}{4}(I_1)^2 + (\tfrac{1}{2})I_1 I_4]^{1/2} \tag{16}$$

and

$$\hat{I}_4 = (\tfrac{1}{2})(I_1 - I_4) - [(\tfrac{1}{2})I_2 - I_5 + \tfrac{1}{4}(I_4)^2 - \tfrac{1}{4}(I_1)^2 + (\tfrac{1}{2})I_1 I_4]^{1/2} \tag{17}$$

Considering a uniformly stressed volume, or, in the context of Weibull analysis, a single link, the invariant $\hat{I}_2$ corresponds to the magnitude of the stress component in the direction of d_i, as shown in Fig. 11.1. $\hat{I}_2$ corresponds to the shear stress on the face normal to d_i. The invariants $\hat{I}_3$ and $\hat{I}_4$ are the

maximum and minimum normal stresses in the plane of isotropy. Note that these physical mechanisms are independent of I_3, and the implication of this is discussed in the following section. Taking

$$\psi = \psi(\hat{I}_1, \hat{I}_2, \hat{I}_3, \hat{I}_4) \tag{18}$$

ensures ψ is form invariant.

At this point it is assumed that the stress components identified by the invariants above act independently in producing failure. Following reasoning similar to Wetherhold[19]

$$\psi = \left[\frac{<\hat{I}_1>}{\beta_1}\right]^{\alpha} + \left[\frac{<\hat{I}_2>}{\beta_2}\right]^{\alpha} + \left[\frac{<\hat{I}_3>}{\beta_3}\right]^{\alpha} + \left[\frac{<\hat{I}_4>}{\beta_3}\right]^{\alpha} \tag{19}$$

It is further assumed that compressive stresses associated with $\hat{I}_1$, $\hat{I}_3$ and $\hat{I}_4$ do not contribute to failure so that

$$<\hat{I}_1> = \begin{cases} \hat{I}_1 & \hat{I}_1 > 0 \\ 0 & \hat{I}_1 \leq 0 \end{cases} \tag{20}$$

$$<\hat{I}_3> = \begin{cases} \hat{I}_3 & \hat{I}_3 > 0 \\ 0 & \hat{I}_3 \leq 0 \end{cases} \tag{21}$$

and

$$<\hat{I}_4> = \begin{cases} \hat{I}_4 & \hat{I}_4 > 0 \\ 0 & \hat{I}_4 \leq 0 \end{cases} \tag{22}$$

Again, the implications of this assumption are discussed in the next section. In addition,

$$<\hat{I}_2> = |\hat{I}_2| \tag{23}$$

for all values of $\hat{I}_2$.

In association with each invariant, the α values correspond to the Weibull shape parameters and the β values correspond to Weibull scale parameters. A two-parameter Weibull probability density function has the following form

$$p(x) = \left[\frac{\alpha}{\beta}\right]\left[\frac{x}{\beta}\right]^{(\alpha-1)} \exp\left[-\left[\frac{x}{\beta}\right]^{\alpha}\right] x > 0 \tag{24}$$

and

$$p(x) = 0 \quad x \leq 0 \tag{25}$$

The cumulative distribution function is given by

$$P(x) = 1 - \exp\left[-\left[\frac{x}{\beta}\right]^{\alpha}\right] \quad x > 0 \tag{26}$$

and

$$P(x) = 0 \quad x \leq 0 \tag{27}$$

where $\alpha(>0)$ is the Weibull modulus (or the shape parameter), and $\beta(>0)$ is the Weibull scale parameter.

Note that $\hat{I}_3$ and $\hat{I}_4$ are stress components in the plane of isotropy and, therefore, have the same Weibull parameters. The parameters α_1 and β_1 would be obtained from uniaxial tensile experiments along the material orientation direction, d_i. The parameters α_2 and β_2 would be obtained from torsional experiments of thin-walled tubular specimens where the shear stress is applied across the material orientation direction. The final two parameters, α_3 and β_3, would be obtained from uniaxial tensile experiments transverse to the material orientation direction.

Insertion of Eqn. (19) into Eqn. (4) along with Eqn. (20) through Eqn. (23) yields a noninteractive reliability model for a three-dimensional state of stress in a transversely isotropic whisker-reinforced ceramic composite. The noninteractive representation of reliability for orthotropic ceramic composites would follow a similar development. The analytical details for this can be found in Duffy and Manderscheid.[20]

Figure 11.2A depicts level surfaces of R (for a uniformly stressed element of unit volume) projected onto the σ_{11}–σ_{33} stress plane for the special case where $d_i = (1.0,0)$, It is assumed that the whiskers are highly aligned along the 1-axis, and the 2–3 plane is the plane of isotropy as shown in Fig. 11.1. Here $\alpha_1 = 15$, $\beta_1 = 700$, $\alpha_2 = 12$, $\beta_2 = 600$, $\alpha_3 = 10$, and $\beta_3 = 500$. The three surfaces correspond to $R = 0.95$, 0.5 and 0.05. Note that the contours of reliability are not symmetric about the line $\sigma_{11} = \sigma_{33}$. The intercepts for the various contours are larger in value along the σ_{11} axis. This increase in reliability results from the alignment of whiskers relative to the load direction (i.e., the direction of σ_{11} and d_i are coincident). Contrast this with the contours of R depicted in Fig. 11.2B. Here the Weibull parameters are unchanged but the orientation of d_i is rotated 45° in the 1–3 plane, thus $d_i = (1/\sqrt{2},0,1/\sqrt{2})$. A comparison of Fig. 11.2A and Fig. 11.2B reveals that the tensile intercepts along both axes increase. An increase in the tensile intercepts along the σ_{33} axis is expected. However, an increase of the tensile intercepts along the σ_{11} axis needs explanation. Consider a flaw located in the material that is initially oriented such that the application of σ_{11} would cause Mode I crack propagation. Upon encountering the aligned whiskers, the flaw deflects in the direction of the whiskers (assuming weak bonding between whisker and matrix) or away from the whiskers (see Faber and Evans[6]). In either case, further propagation would proceed under mixed mode conditions and requires an increase in σ_{11}. This is reflected in an increase of the intercepts along the axes. A further consideration of Fig. 11.2B shows that for equibiaxial compression, reliability is unity. Expansion of the invariants under these conditions would result in all four invariants being equal to zero.

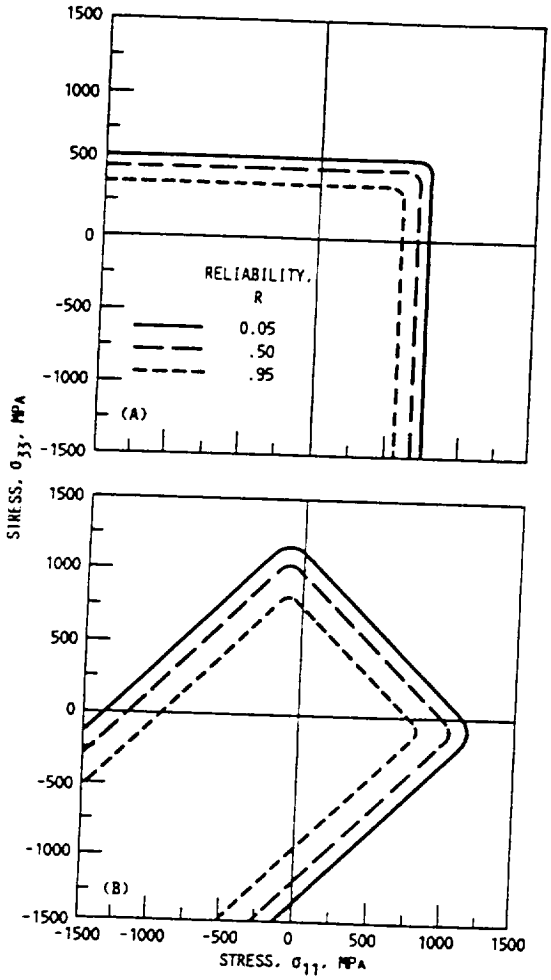

Fig. 11.2 Typical family of reliability contours. Weibull parameters, $\alpha_1 = 15$, $\beta_1 = 700$, $\alpha_2 = 12$, $\beta_2 = 600$, $\alpha_3 = 10$, and $\beta_3 = 500$. Contours shown with (A) local material direction coincident with σ_{11}, and (B) effect of rotating the local material direction 45° in the 1–3 plane.

11.2.3 Interactive Reliability Model

An essential step in developing an interactive reliability model requires formulating a deterministic failure criterion that reflects the limit state behavior of the material. Miki *et al.*,[21] and de Roo and Paluch[22] have adopted this approach in computing the reliability of unidirectional composites. In both articles, the Tsai–Wu failure criterion is adopted, where different failure behavior is allowed in tension and compression, both in the fiber direction and

transverse to the fiber direction. Here, the authors assume that failure behavior for isotropic whisker-toughened ceramics will exhibit a reduced tensile strength in comparison to the material's compressive strength, and exhibit a dependence on the hydrostatic component of the stress state. This behavior has not been documented experimentally in the open literature, but this type of response has been exhibited by monolithic ceramics, and we have similar expectations for the whisker-toughened ceramics.

In general, a failure criterion (or limit state) defines the conditions under which a structural component can no longer fulfill its design function. Let

$$\vec{Y} = (Y_1, Y_2, \ldots, Y_n) \tag{28}$$

denote a vector of design variables (e.g., strength parameters, cyclic load limits, allowable deformation at critical locations of a component, etc.). A limit state function $f(\vec{Y})$, which stipulates how the design variables interact to produce failure, defines a surface in the n-dimensional design variable space. Typically, the following simple expression

$$f(\vec{Y}) = 0 \tag{29}$$

is used to define the failure surface. A design point for a structural component that falls within the surface defines a successful operational state. This region will be denoted ω_s. If the design point lies on the surface (denoted ω_f), the component fails. Note that points outside the failure surface are inaccessible limit states. Here, we restrict the design variable space to material strength parameters. These material strength parameters will be closely associated with components of the stress tensor, hence, in general

$$f = f(\vec{Y}, \sigma_{ij}) \tag{30}$$

where σ_{ij} represents the Cauchy stress tensor. As was discussed in the previous section, due to the dependence upon the stress tensor, phenomenological failure criteria must be formulated as invariant functions of σ_{ij}. Using this approach makes a criterion independent of the coordinate system used to define the stress tensor (i.e., the criterion exhibits frame indifference). In general, for isotropic materials the failure function can be expressed as

$$f(\vec{Y}, I_1, J_2, J_3) = 0 \tag{31}$$

which guarantees that the function is form invariant under all proper orthogonal transformations. Here I_1 is the first invariant of the Cauchy stress defined by Eqn. (9), J_2 is the second invariant of the deviatoric stress (S_{ij}), and J_3 is the third invariant of the deviatoric stress. These quantities are defined in the following manner

$$S_{ij} = \sigma_{ij} - (1/3)\,\delta_{ij}\sigma_{kk} \tag{32}$$

$$J_2 = (1/2)\,S_{ij}S_{ji} \tag{33}$$

$$J_3 = (1/3)\,S_{ij}S_{jk}S_{ki} \tag{34}$$

where δ_{ij} is the identity tensor. Admitting I_1 to the functional dependence allows for a dependence on hydrostatic stress. Admitting J_3 (which changes sign when the direction of a stress component is reversed) allows different behavior in tension and compression to be modeled with a single unified failure function.

Two representative failure criteria formulated by Willam and Warnke,[23] and Ottosen[24] satisfy the requisite failure behavior of reduced tensile strength, and sensitivity to hydrostatic stress. For the sake of brevity, the discussion here is limited to the Willam–Warnke criterion. The Willam–Warnke criterion can be expressed as

$$f = \lambda\left[\frac{\sqrt{J_2}}{Y_c}\right] + B\left[\frac{I_1}{Y_c}\right] - 1 \tag{35}$$

where

$$B = B(Y_t, Y_c, Y_{bc}) \tag{36}$$

and

$$\lambda = \lambda(Y_t, Y_c, Y_{bc}, J_3) \tag{37}$$

Here Y_t denotes the tensile strength of the material, Y_c is the compressive strength, and Y_{bc} represents equal biaxial compression strength of the material. The reader is directed to Palko[25] where the specific forms of B and λ are presented. This model is termed a three-parameter model, referring to the three material strength parameters (Y_t, Y_c, and Y_{bc}) used to characterize the model. Failure is defined when $f = 0$, and the multiaxial criterion is completely defined in the six-dimensional stress space.

The general nature of the criterion can be examined by projecting the failure function into various coordinate systems associated with the applied stress state. In Fig. 11.3 the function has been projected onto the principal stress plane, i.e., the σ_1–σ_2 stress plane. Note that this plane coincides with the σ_{11}–σ_{22} stress plane. Here the model parameters have been arbitrarily chosen ($Y_t = 0.2$, $Y_c = 2.0$, and $Y_{bc} = 2.32$). Note that the reduction in tensile strength, and the ratio of intercepts along the tensile and compressive axes, is equal to the ratio of Y_t to Y_c. The functional dependence of the limit state function governed by the Willam–Warnke criterion is given by

$$f(\bar{Y}, \sigma_{ij}) = f(Y_t, Y_c, Y_{bc}, I_1, J_2, J_3) \tag{38}$$

where the specific form of $f(\bar{Y}, \sigma_{ij})$ is given by Eqn. (35). It is assumed that the material strength parameters are independent random variables. The objective is to compute the reliability (denoted $\mathcal{R}$) of a material element of unit volume, given a stress state, where the components of the stress tensor are considered deterministic parameters. This philosophy, i.e., assuming that material strength parameters are independent random variables and load parameters are deterministic, is not without precedent. The reader is directed to the overview

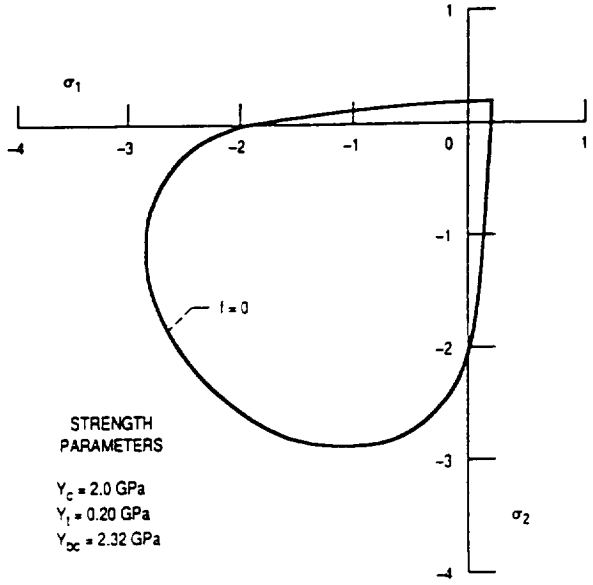

Fig. 11.3 Level failure surface ($f = 0$) of the Willam and Warnke failure criterion projected onto the σ_1–σ_2 stress plane.

by Duffy *et al.*[26] for references. The reliability of the ith element of a structural component is given by the following expression

$$\mathcal{R}_i = \text{Probability}[f(\tilde{Y}) < 0] \tag{39}$$

Under the assumption that the random variables are independent, this probability is given by the product of the marginal probability density functions integrated over the region ω_s, i.e.,

$$\mathcal{R}_i = \int \int_{\omega_s} \int p_1(y_c) p_2(y_t) p_3(y_{bc})\, dy_c\, dy_t\, dy_{bc} \tag{40}$$

where $p_1(y_c)$, $p_2(y_t)$, and $p_3(y_{bc})$ are the marginal probability density functions of the random variables representing the material strength parameters. Here, the two-parameter Weibull formulation, defined by Eqn. (24) and Eqn. (25), is used for the probability density function. A feature of this analytical approach is the flexibility of using other formulations of the marginal probability density function, such as a three-parameter Weibull distribution or a log–normal distribution. The appropriate distribution function would be dictated by the experimental failure data for a particular strength parameter. Here, for the purposes of illustration, the two-parameter Weibull distribution is adopted for simplicity.

Explicit integration of Eqn. (40) is intractable due to the form of the limit state function which defines the integration domain (ω_s). The reader is referred

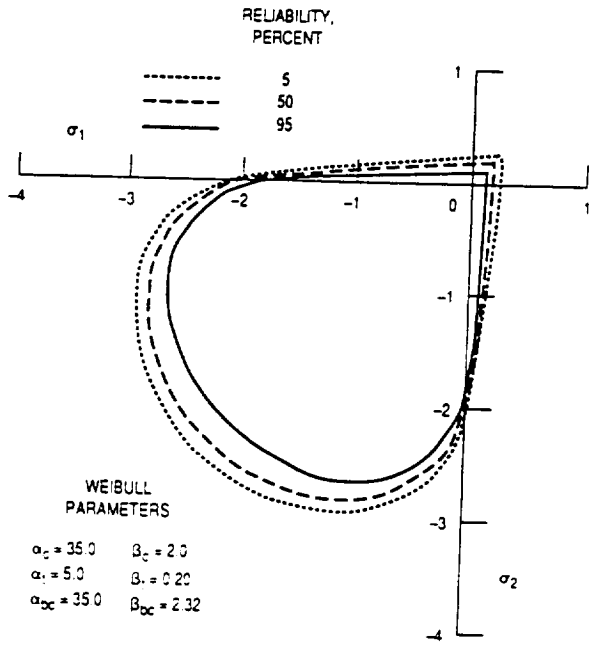

Fig. 11.4 Family of reliability contours associated with an interactive reliability model projected onto the σ_1–σ_2 stress plane.

to Sun and Yamada,[27] and Wetherhold[19] for the details of this type of integration for simpler interactive failure criteria. Here, Monte Carlo simulation is used to numerically evaluate the triple integral. This technique involves generating a uniform random sample of size k for each of the random variables. For a given stress state, the failure function is computed for each trial sample of random variables. If $f(\tilde{Y}) < 0$ for a given trial, then that trial is recorded as a success. By repeating this process a suitable number of times for a given state of stress, a probability distribution for the element reliability is generated. For a sufficiently large sample size, reliability can be computed as

$$\mathcal{R}_i = n/k \tag{41}$$

where n is the number of trials where $f(\tilde{Y}) < 0$.

This technique was employed in calculating the reliability contours depicted in Fig. 11.4. The reliability contours represent a homogeneously stressed material element, and for dimensionless $\mathcal{R}_i$, the Weibull parameter β has units of stress·(volume)$^{1/\alpha}$. Here $\alpha_t = 5$, $\beta_t = 0.2$, $\alpha_c = 35$, $\beta_c = 2$, $\alpha_{bc} = 35$, and $\beta_{bc} = 2.32$. The three surfaces correspond to $\mathcal{R}_i = 0.95$, 0.5, and 0.05. Note that the reliability contours retain the general behavior of the deterministic failure surface from which they were generated. In general, as the α values increase, the spacing between contours diminishes. Eventually the contours would not be distinct and they would effectively map out a

deterministic failure surface. An increase in the β values shifts the relative position of the contours in an outward direction.

The noninteractive and interactive reliability models discussed above have been incorporated into a public domain computer algorithm given the acronym T/CARES (Toughened Ceramics Analysis and Reliability Evaluation of Structures). The reliability analysis of a structural component requires that the stress field must be characterized. Commercial finite element programs allow the design engineer to determine the structural response of composite components subjected to thermomechanical loads. Currently, this algorithm is coupled to the MSC/NASTRAN finite element code. For a complete description of the algorithm, see Duffy *et al.*[12] Before utilizing T/CARES, the reliability models presented here (and later in this chapter) must be characterized using an extensive database that includes multiaxial experiments. It is not sufficient to simply characterize the Weibull parameters for each strength parameter. Multiaxial experiments should be conducted to assess the accuracy of the interactive modeling approach. However, once the Weibull parameters have been characterized for each strength variable, the computer algorithm allows a design engineer to predict the reliability of a structural component subject to quasi-static multiaxial loads. Note that the algorithm is capable of nonisothermal analyses if the Weibull parameters are specified at a sufficient and appropriate number of temperature values.

11.3 Laminated Ceramic Matrix Composites

11.3.1 Introduction

Although whisker-reinforced ceramics have enhanced toughness and reliability, they do not substantially lessen the possibility of catastrophic failure, a problem that restricts their use in certain applications. Continuous fiber-reinforced ceramic composites, however, can provide significant increases in fracture toughness along with ability to fail in a noncatastrophic manner (often referred to as "graceful" failure). Prewo and Brennan[28–30] have demonstrated that incorporating fibers with high strength and stiffness into brittle matrices with similar coefficients of thermal expansion and optimized interfaces yields ceramic composites with the potential of meeting high temperature performance requirements. Typical stress–strain curves of unidirectional systems (see Fig. 11.5) tend to be bilinear when loaded along the fiber direction, with a distinct breakpoint that usually corresponds to the formation of an initial transverse matrix crack. From Fig. 11.5 it is somewhat apparent that an engineer may focus attention on three factors when designing components fabricated from ceramic matrix composites. They are:

(1) the stress (or strain associated with the formation of the first transverse matrix crack (often referred to as the microcrack yield strength);

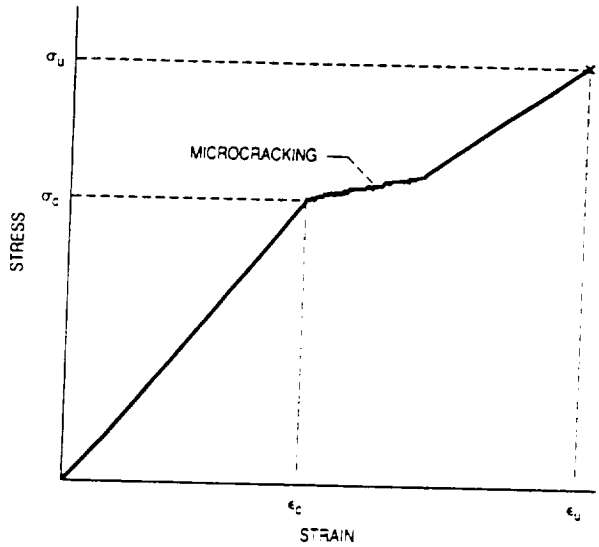

Fig. 11.5 Generic stress–strain curve for a unidirectional ceramic matrix composite with a tensile load imposed in the fiber direction.

(2) the stress (or strain) associated with the ultimate strength of the material: and
(3) the work of fracture, associated with the total area under the stress–strain curve.

Which design factor is of primary importance will depend on the application of the structural component. If limiting strength degradation during the life of a component is important, then the transverse matrix cracking stress becomes the design focus. This restricted focus limits full exploitation of the ultimate load carrying capacity of the material. However, adopting this viewpoint should extend the life of a component since the matrix serves as protection for the fibers and the interface, shielding them from high temperature service environments that cause oxidation and rapid degradation in composite strength. If life is not an important design issue (e.g., the turbine components used in a single-mission cruise missile) then the engineer may extend the design envelope past first matrix cracking and utilize more of the ultimate strength of the composite. In either case, a component benefits from the increase in work of fracture which is a measure of the graceful failure behavior associated with unidirectional reinforced ceramic composites.

Theoretically, the addition of a ceramic fiber to a ceramic matrix should increase strength (both microcrack yield and the ultimate) *and* fracture toughness. Traditionally, fiber reinforcement has been employed to strengthen a matrix with a low modulus and low strength, by transferring load to high modulus, high strength fibers. This type of transfer mechanism demands a

microstructure with reasonably strong bonding at the interface between the matrix and the fiber. The result is a composite with fiber-dominated failure behavior. To date, ceramic composite microstructures that promote increased toughness (mainly due to fiber pull-out) have usually done so at the expense of the microcrack yield strength. In the presence of an interface that is too strongly bonded, a transverse matrix crack merely propagates through both the fiber and the matrix in a self-similar fashion. In essence, monolithic failure behavior is obtained. Since catastrophic fracture is the overriding concern with monolithic ceramics, fibers are added to mitigate tensile failure by bridging flaws, and this requires a weakly bonded interface. As a consequence of a weak interface, a transverse matrix crack encounters the interface, changes direction and debonds along the fiber. The applied far-field stress must then be increased for further self-similar crack extension, thus the toughness of the material is increased. The lack of improvement in the first matrix cracking strength of continuous fiber-reinforced ceramic matrix composites is a direct result of current fabrication processes that do not yield optimized interfaces and uniform matrix densities. As fabrication technologies evolve and fully dense matrices with high fiber volumes become a reality, composite matrix cracking strength should also improve.

11.3.2 Reliability Issues

Relative to component reliability, current state of the art focuses on composite tensile strength in the fiber direction, which addresses the upper bound problem. Conversely, a tensile load applied transverse to the fiber direction results in failure behavior similar to, or worse than, a monolithic ceramic. This represents the lower bound of composite strength. The transverse direction also does not possess the graceful failure behavior, and for this reason (and since the majority of structural applications involve multiaxial states of stress) practical continuous fiber composites are reinforced in two or three directions using laminated, woven, or braided architectures. Two-dimensional laminate construction is the focus in this section.

As is indicated throughout this chapter, there is a philosophical division that separates analytical schools of thought for predicting failure behavior into micro- and macro-level methods. Blass and Ruggles[31] point out that analysts from the first school would design the material in the sense that the constituents are distinct structural components, and the composite ply (or lamina) is considered a structure in its own right. Analysts from the latter school of thought would design with the material, i.e., analyze structural components fabricated from the material. Since failure (assuming that deformation or stability does not control component design) usually emanates from crack-like defects in most brittle materials, it is not unreasonable to apply the principles of fracture mechanics to ceramic composite systems. There is a wealth of literature concerning the application of linear elastic fracture mechanics (LEFM) to many types of composite materials. The reader is

directed to the volume edited by Friedrich[32] for a state-of-the-art review on this topic. If a unidirectional composite is treated as a homogenized material using fracture mechanics, then the details of the microstructure are ignored. Usually the ply is treated as an anisotropic plate and the approach is used to predict failure loads when notches or holes are present in a structure. However, problems arise with this approach when obtaining critical stress intensity factors and/or critical strain energy release rates in composites where self-similar crack growth is an experimental myth. In addition, since failure in ceramic composites is sensitive to flaws and geometric discontinuities at a much smaller scale, this approach has not found many proponents in the past.

The alternative is to account for the details of the microstructure, since it is typical to assume that the size of critical flaws is of the same order of magnitude as the characteristic dimensions of the microstructure (e.g., fiber diameter, crack spacing). Rigorous fracture mechanics criteria that adopt the microstructural viewpoint have been proposed to predict first matrix cracking (e.g., Budiansky *et al.*,[33] and Marshall *et al.*[34]), yet these approaches make the rather strong simplifying assumption that the analyst has a working knowledge of the constituent properties, constituent geometries, and arrangements. This is simplistic, especially in light of the mechanical properties of the interface. The authors wish to point out that different types of pull-out and push-out tests have been advocated to characterize interfacial shear properties. With these experiments, assumptions must be made concerning the stress distribution in the interface along the fiber length. A uniform interface is universally assumed (along with the various postulated stress distributions) which is rather remarkable since post-failure investigations of typical CMC microstructures usually indicate that the interface is highly nonuniform, or even totally absent. Current fabrication technology does not produce a consistent interface in most ceramic composites. This strongly indicates that stochastic approaches should be considered in characterizing the strength of unidirectional ceramic composites. If probabilistic methods are utilized, then the reader will notice in the previous discussion, and in what follows, that employing reliability analyses requires the design engineer to characterize the state of stress throughout the component. Local–global techniques will not work since component probability of failure is computed based on the reliability of each discrete element. Using finite element techniques at the constituent level to characterize the stress state of an entire component would quickly exhaust the capacity of a supercomputer. Thus, conducting component failure analyses at the microstructural level using fracture mechanics is not a viable design alternative.

As a final note regarding the use of fracture mechanics, several authors have combined fracture mechanics with a probabilistic Weibull analysis of fiber failure to determine the stress–strain behavior and subsequent work of fracture for unidirectional composites (e.g., Thouless and Evans,[35] and Sutcu[36]). However, the focus here is on first matrix cracking, i.e., designing composite structures for extended service life. We note that mature reliability-based design methods using fracture mechanics concepts will not surface until a

coherent mixed mode fracture criterion has been proposed that accounts for complex crack geometries, fiber/matrix debonding, and closing pressures resulting from fibers that bridge highly irregular matrix cracks. Even when the state of the art reaches this point, fracture mechanics may have a practical utility in designing the material, but not a component.

If component failure analyses based on fracture mechanics are not the answer, the engineer can turn to design methods based on phenomenological strength models. As in fracture mechanics, phenomenological models can be proposed at the macrostructural and microstructural levels. The authors advocate the school of thought mentioned above which idealizes the ply (or lamina) as a homogenized material with strength properties that are determined from phenomenological experiments. There are practical reasons for embracing this viewpoint. The authors fully recognize that the failure characteristics of these composites are controlled by a number of local phenomena including matrix cracking, debonding and slipping between matrix and fibers, and fiber breakage, all of which strongly interact. Understanding the underlying analytical concepts associated with the microstructural viewpoint allows one to gain insight and intuition prior to constructing multiaxial failure theories that, in some respect, reflect the local behavior. However, proposing phenomenological models at the microstructural level entails developing an extensive property database that must include all the constituents. As noted earlier, constituent properties are not often uniform throughout the microstructure. A top-down approach, that is first proposing analytical models at the ply level, will establish viable and working design protocols. Initially adopting the bottom-up approach allows for the possibility of becoming mired in detail (experimental and analytical) when multiaxial reliability analyses are conducted at the constituent level.

Size effect (i.e., decreasing bulk strength with increasing component size) is an important feature of ceramic composites that must be addressed in failure analysis. How it is addressed depends on whether the material is modeled as a series system, a parallel system, or a combination. Current analytical practice uses finite element methods to determine the state of stress throughout the component. It is assumed that failure is dependent upon the stress state in a component, such that deformations are not controlling design. Since failure may initiate in any of the discrete volumes (elements), it is useful to consider a component as a system. A component comprised of discrete volumes is a series system if it fails when one of the discrete volumes fails. This approach gives rise to weakest-link theories. In a parallel system, failure of a single element does not dictate that the component has failed, since the remaining elements may be able to sustain the load through redistribution. Adopting a parallel system approach leads to what has been referred to in the literature as bundle theories.

The basic principles of bundle theory were originally discussed by Daniels[37] and Coleman.[38] Their work was extended to polymer matrix composites by Rosen[39] and Zweben.[40] Here, a relatively soft matrix serves to

transfer stress between fibers, and contributes little to the composite tensile strength. Hence, when a fiber breaks, the load is transferred only to neighboring fibers. Their analysis is rather complex and limited to establishing bounds on the stress at which the first fiber breaks and the stress at which all the fibers are broken. Harlow and Phoenix[41] proposed a rather abstract approach that established a closed-form solution for all the intermediate stress levels in a two-dimensional problem, and Batdorf[42] used an approximate solution to establish the solutions for the three-dimensional problem. Batdorf's model includes the two-dimensional model as a special case. In both of the latter two models, the concept of an effective Weibull modulus that increases with increasing component volume is proposed. This implies a diminished size effect. However, these current bundle theories are predicated on the fact that fibers are inherently much stronger and stiffer than the matrix. In laminated CMC materials this is not always the case. The magnitudes of the fiber and the matrix stiffness are usually close in value while fiber strength is usually much higher due to the small fiber size effect. Since fiber bundle ultimate strength theories are discussed elsewhere in this book, they will not be considered in this chapter.

The authors advocate the use of a weakest link reliability theory in designing components manufactured from laminated CMC materials that exhibit a limited size effect in specific directions. Assuming that a laminated structure behaves in a weakest link manner allows the calculation of a conservative estimate of structural reliability. Provided that appropriate failure data are used, Thomas and Wetherhold[43] point out that this is also consistent with predicting the probability of the first matrix crack occurring in an individual ply, either in the longitudinal or transverse directions. For most applications, the design failure stress for a laminated material will be taken to coincide with this event (i.e., first ply matrix cracking). The reason for this is that matrix cracking usually leads to high temperature oxidation of the interface and consequent embrittlement of the composite.

11.3.3 Laminate Reliability Model

There is a great deal of intrinsic variability in the strength of each brittle constituent of a ceramic matrix composite, but depending on the composite system, the first matrix cracking strength and the ultimate strength may either be deterministic or probabilistic. Statistical models are a necessity for those composite systems which exhibit appreciable scatter in either of these. Here, we focus on first matrix cracking and treat it in a probabilistic fashion, requiring that deterministic strength be a limiting case that is readily obtainable from the proposed reliability model. With regard to high temperature service conditions, the reader should keep in mind that the parameters associated with the reliability models presented in this section are temperature dependent. In a sense, this is analogous to taking the stiffness parameters in linear elasticity to be temperature dependent. The structure of the reliability models does not

change with service temperature, but the model parameters and component reliability do.

Predicting the reliability due to loads in the fiber direction addresses an upper bound for ply reliability in a structural design problem. Conversely, a tensile load applied transverse to the fiber direction results in failure behavior similar to a monolithic ceramic, which corresponds to the lower bound of ply reliability. Thus, multiaxial design methods must be capable of predicting these two bounds as well as accounting for the reduction in reliability due to an in-plane shear stress, and compressive stresses in the fiber direction and transverse to the fiber direction. The reader should also be cognizant of the delamination failure mode, and for relatively thick laminates, failure may emanate from out-of-plane stresses; however, neither will be addressed in what follows. A number of macroscopic theories exist that treat unidirectional composites as homogenized, anisotropic materials, assuming a plane state of stress. These methods use phenomenological strength data directly without hypothesizing specific crack shapes or distributions. Theories of this genre are generally termed noninteractive if individual stress components are compared to their strengths separately. In essence, failure modes are assumed not to interact and this results in component reliability computations that are quite tractable. Noninteractive models mentioned in the previous section dealing with whisker-toughened composites, as well as work by Thomas and Wetherhold,[43] are representative of multiaxial noninteractive reliability models for anisotropic materials. In addition Wu,[44] and Hu and Goetschel[45] have proposed simpler unidirectional reliability models for laminated composites that can be classified as noninteractive. Alternatively, one can assume that for multiaxial states of stress, failure modes interact and depend on specific stochastic combinations of material strengths. The reader is directed to an excellent generic treatment of this approach by McKernan.[46] Failure modes can be either identified and characterized by micromechanics (see McKernan[46]), or a phenomenological failure criterion is adapted from existing polymer matrix design technologies. The probability that the criterion has been violated for a given stress state is computed using Monte Carlo methods,[21] or first-order–second-moment (FOSM) methods.[22] For the sake of brevity only the noninteractive approach is presented here.

A noninteractive phenomenological approach is presented where a unidirectional ply is considered a two-dimensional structure in a state of plane stress which is assumed to have five basic strengths (or failure modes). They include a tensile and compressive strength in the fiber direction, a tensile and compressive strength in the direction transverse to the fiber direction, and an in-plane shear strength. In addition, each ply is discretized into individual sub-ply volumes. For reasons discussed in the previous section, we assume that failure of a ply is governed by its weakest link (or sub-ply volume). Under this assumption, events leading to failure of a given link do not affect other links (see, for example, Batdorf and Heinisch,[47] Wetherhold,[19] and Cassenti[14]):

thus, the reliability of the ith ply is given by the following expression

$$R_i = \exp\left[- \int_V \psi_i dV \right] \tag{42}$$

Here, $\psi_i(x_j)$ is the failure function per unit volume at position x_j within the ply, given by

$$\psi_i = \left[\frac{<\sigma_1 - \gamma_1>}{\beta_1} \right]^{\alpha_1} + \left[\frac{|\tau_{12} - \gamma_2|}{\beta_2} \right]^{\alpha_2} + \left[\frac{<\sigma_2 - \gamma_3>}{\beta_3} \right]^{\alpha_3} + \\ + \left[\frac{<(-1)(\sigma_1 + \gamma_4)>}{\beta_4} \right]^{\alpha_4} + \left[\frac{<(-1)(\sigma_2 + \gamma_5)>}{\beta_5} \right]^{\alpha_5} \tag{43}$$

where V is the component volume. The α values associated with each term in Eqn. (43) correspond to the Weibull shape parameters, the β values correspond to Weibull scale parameters, and the γ values correspond to the Weibull threshold stresses. In addition, σ_1 and σ_2 represent the in-plane normal stresses that are aligned with, and transverse to, the fiber direction, respectively. Also, τ_{12} is the in-plane shear stress. Normal stresses appear twice and this allows for different failure strengths to emerge in tension and compression. Note that the brackets indicate a unit step function, i.e.,

$$<x> = x \cdot u[x] = \begin{cases} x & x > 0 \\ 0 & x \leq 0 \end{cases} \tag{44}$$

The reader should note that Weibull threshold parameters were employed in Eqn. (43). Thus, it is assumed that each random strength variable is characterized by a three-parameter Weibull distribution. This is a broad (but a less restrictive) assumption that necessitates some reflection. First, not enough failure data exist to completely characterize an existing CMC material system. However, the experience that monolithic ceramics occasionally exhibit threshold behavior (see Duffy *et al.*,[48] and Margetson and Cooper[49]), combined with the fact that one would intuitively assume that threshold behavior would occur in the fiber direction, indicates that this issue should be approached with an open mind. Estimation techniques have been proposed by numerous authors, and the reader is directed to Duffy *et al.*[50] for an overview.

Inserting Eqn. (43) into the volume integration given by Eqn. (42) yields the reliability of the ith ply, and the probability of first ply failure for the laminate is given by the expression

$$P_{fpf} = 1 - \prod_{i=1}^{N} R_i \tag{45}$$

where N is the number of plies. The computation given in Eqn. (45) represents an upper bound on component probability of failure. Alternatively, Thomas

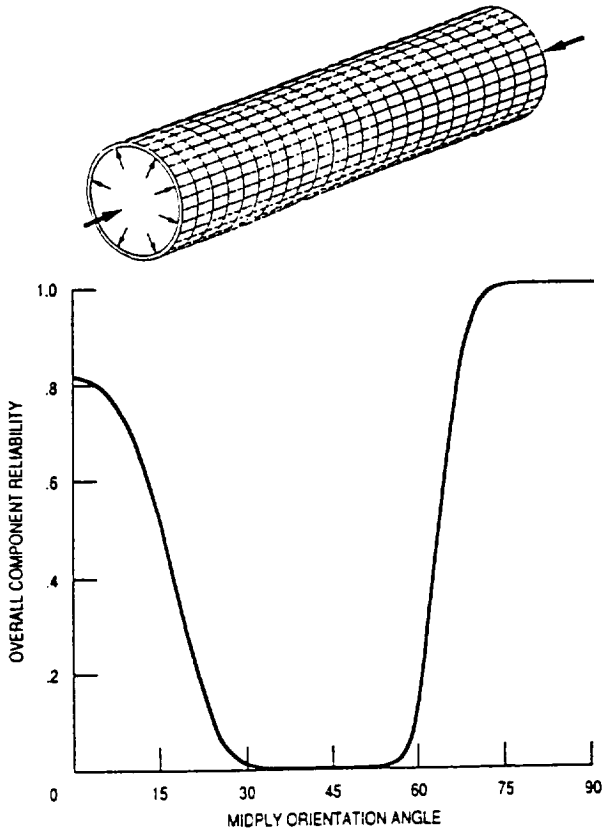

Fig. 11.6 Finite element mesh of a thin-walled tube with an imposed internal pressure and axial compressive stress. Component reliability is plotted as a function of the mid-ply orientation angle.

and Wetherhold[43] proposed a lower bound on component probability of failure by assuming the failure behavior of a component is dominated by the strongest link in the chain. Failure does not occur until the strongest link has failed. Component probability of failure is obtained by subtracting the product of probabilities of failure of each ply from unity, i.e.,

$$(P_f)_{lower} = \prod_{i=1}^{N} (1 - R_i) \tag{46}$$

Either reliability model can be readily integrated with laminate analysis options available in several commercial finite element codes. A preliminary version of a public domain computer algorithm (C/CARES)[48] has been coupled with MSC/NASTRAN to perform this analysis. A simple benchmark application illustrates the approach. A thin-walled tube is subjected to an internal pressure and an axial compressive load. The component is fabricated from a

Table 11.1 Composite Weibull parameters for thin-walled tube (Weibull threshold stress, $\gamma_i \equiv 0$)

Index[a]	*Type and direction of stress*	*Weibull parameters*	
		Shape (α_i)	*Scale* (β_i)
1	Normal tensile stress in fiber direction	25	450
2	In-plane shear stress	22	420
3	Normal tensile stress transverse to fiber direction	10	350
4	Normal compressive stress in fiber direction	35	4500
5	Normal compressive stress transverse to fiber direction	30	3500

[a] Indices correspond to subscripts in Eqn. (43).

three-ply laminate, with a $90°/\theta/90°$ lay-up. Here, angle θ is measured relative to the longitudinal axis of the tube (see Fig. 11.6). An arbitrary internal pressure of 4.25 MPa and axial compressive stress of 87.5 MPa were applied to the tube. The Weibull parameters were also arbitrarily chosen (see Table 11.1). Indices 1 and 4 from Table 11.1 are associated with the normal stress (tensile and compressive, respectively) in the fiber direction. Similarly, indices 3 and 5 are associated with the normal stress (tensile and compressive, respectively) transverse to the fiber direction. Finally, index 2 is associated with the in-plane shear stress. Note that the threshold stresses are taken equal to zero for simplicity. In design, setting the threshold stresses equal to zero would represent a conservative assumption. The overall component reliability is depicted as a function of the mid-ply orientation angle (θ) in Fig. 11.6. This illustrates that ply orientation has a decided effect on component reliability, as expected. Similar studies can be conducted that demonstrate the effect that component geometry, ply thickness, load, and/or Weibull parameters have on component reliability. Hence, the C/CARES code allows the design engineer a wide latitude to optimize a component relative to a number of design parameters.

11.4 Fabric-Reinforced Ceramic Matrix Composites

Advancements in textile weaving technology have resulted in significant new opportunities for utilizing high performance two- and three-dimensional fabric-reinforced ceramic matrix composites in high temperature structural applications (see Fareed *et al.*,[51] and Ko *et al.*[52]). Attractive features include improvements in damage tolerance and reliability, flexibility in fiber placement

and fabric architecture, and the capability of near-net-shape fabrication. This latter feature is of particular interest since applications where these materials can make a significant impact often require complex geometric shapes. However, designing structural components that are fabricated from materials incorporating ceramic fiber architectures also represents new and distinct challenges in analysis and characterization. Preforms, which serve as the composite skeleton, are produced by weaving, knitting and braiding techniques (see Ko[53]). Woven fabrics (i.e., two-dimensional configurations) exhibit good stability in the mutually orthogonal warp and weft directions. Triaxially woven fabrics, made from three sets of yarns which interlace at 60° angles, offer nearly isotropic behavior and higher out-of-plane shearing stiffness. A three-dimensional fabric, consisting of three or more yarn diameters in the thickness direction, is a network where yarns pass from fabric surface to fabric surface. These three-dimensional systems can assume complex shapes and provide good transverse shear strength, impact resistance, and through-the-thickness tensile strength. Furthermore, the problem of interlaminar failure is totally eliminated. However, due to crimping of fibers and less than optimized fiber fractions in the primary load direction, some tailoring and optimization is usually sacrificed when compared to traditional laminated composites.

Complex textile configurations and complicated yarn–matrix interface behavior represent a challenge in determining the mechanical properties of these composites. Considerable effort has been devoted to evaluating the effectiveness of various reinforcement architectures based upon approximate geometrical idealizations. Chou and Yang[54] have summarized the results of extensive studies in modeling thermoelastic behavior of woven two-dimensional fabrics, and braided three-dimensional configurations. They proposed a unique method of constructing structure–performance maps, which show anisotropic stiffness variations of angle-ply, cross-ply, fabric and braided-fiber architectures. The relative effectiveness of various textile-reinforcing schemes can be assessed using these maps. In the future, as these materials emerge, the maps should serve as a guide for design engineers wishing to specify these materials.

Several analytical models have been developed to predict the mechanical properties and structural behavior of these composites. The approaches are based mainly on modified laminate theory, and/or a geometric unit cell concept. For two-dimensional woven fabric reinforced composites, Chou and Ishikawa[55] have proposed three models using laminate theory. These models are known as the mosaic, crimp, and bridging models. The mosaic model ignores fiber continuity and treats a fabric composite as an assemblage of cross-ply laminates. The crimp model takes into account the continuity and undulation of the yarns; however, it is only suitable for plain weaves. The bridging model, developed for satin weaves, is essentially an extension of the crimp model. This model takes into consideration the contribution to the total stiffness of the linear and nonlinear yarn segments.

The concept of a geometric unit cell has been widely used to characterize

the complex structure of three-dimensional fiber-reinforced composites and to establish constitutive relations. In general, this approach assumes that the thermoelastic properties are functions of fiber spatial orientation, fiber volume fraction, and braiding parameters. Ma *et al.*[56] developed a fiber interlock model which assumes that the yarns in a unit cell of a three-dimensional braided composite consist of rods which form a parallelepiped. Contribution to the overall strain energy from yarn axial tension, bending, and lateral compression are considered, and formulated within the unit cell. Yang *et al.*[57] proposed a fiber inclination model that assumes an inclined lamina is represented by a single set of diagonal yarns within a unit cell. Ko *et al.*[58] have also proposed a unit cell model where the stiffness of a three-dimensional braided composite is considered to be the sum of the stiffnesses of all its laminae. The unique feature of this model is that it admits a three-dimensional braid as well as the other multidirectional reinforcements, including five-, six-, and seven-directional yarns that are either straight or curvilinear. Finally, Crane and Camponeschi[59] have modeled a multidimensional braided composite using modified laminate theory. Their approach determines the extensional stiffness in the three principal geometric directions of a braided composite. We note that these analytical models are based on previous research related to polymeric and metal matrix composites. Though much of the current stiffness modeling effort is in its infancy, the approaches mentioned above have demonstrated merit relative to experimental data. However, caution is advised since agreement between model predictions and experimental data is subject to interpretation. Yet accurate predictions of mechanical properties are a necessity when conducting stress–strain analyses which logically precede all failure studies.

Recently, characterization studies that focus on the failure behavior of woven ceramic composites have been appearing in the open literature. The work of Wang *et al.*[60] and Chulya *et al.*[61] represents the fundamental type of exploratory test programs necessary in the study of constitutive response and damage mechanisms. It is apparent from these studies that material behavior is dominated by voids and gaps located in the interstices of the weave. Behavior in tension and compression is different. Tensile behavior is influenced by microcracking which is the direct result of residual stresses developed during fabrication. The nonlinear tensile stress–strain curve exhibits a continuous reduction in stiffness in the initial load cycle. However, subsequent load cycles yield relatively linear stress–strain behavior. This indicates that most of the damage accumulation takes place during the initial load cycle. Wang *et al.*[60] postulated that the ultimate tensile strength of woven ceramic composites is governed by the formation of distributed transverse cracks that terminate at voids or fibers in the materials. These transverse cracks eventually link up, causing ultimate failure. Yen *et al.*[62] have proposed a model that accounts for this type of behavior by assuming the formation of H-shaped cracks which eventually merge, leading to ultimate failure. The mechanical response of this material under compressive loads yields nearly linear behavior up to the

ultimate strength. The ultimate compressive strength was associated with buckling of fiber bundles and matrix fragmentation.

Predicting the onset of failure represents a complex task due to the numerous failure modes encountered in this class of materials. As research progresses, deterministic and probabilistic schools of thought will emerge. For either case, models based upon the principles of fracture mechanics, as well as phenomenological models, will be proposed. It is expected that deterministic approaches will precede the development of probabilistic concepts. Initial research regarding failure analysis for whisker-toughened and long fiber ceramic composites typically borrowed concepts from polymer and metal matrix composite research. We anticipate a similar trend with woven composites.[63] For example, Yang,[64] and the previously cited work of Chou and Ishikawa[55] have proposed techniques for predicting the onset of short-term failure in fabric-reinforced polymer composites that make use of the maximum stress and maximum strain failure criteria. The work by Walker *et al.*[65] represents another potential concept that could be utilized. Here, mesomechanics is employed to predict the behavior of metal matrix composites. This approach takes advantage of the periodic nature of the microstructure, and homogenizes the material through volume averaging techniques. In Walker's work, a damage parameter can be included as a state variable in formulating constitutive relationships. Other suitable failure concepts may emerge from the field of continuum damage mechanics as well.

Currently, phenomenological approaches may be the logical first choice due to the complexity of the microstructure. Yet one should be cognizant of the fact that random microcracks and voids are present in woven ceramics. These microdefects may lead to statistically distributed failures and failure modes. However, at this time, failure models based upon probabilistic concepts have not been proposed. A more extensive database is needed to identify the underlying mechanisms of failure, and innovative experimental techniques must accompany the development of constitutive models that incorporate damage evolution at the microstructural level. The task will be iterative, requiring constant refinement of the description of the physical mechanisms causing failure and their mathematical description. The authors wish to point out that fiber preform design, constitutive modeling, and material processing, will require the combined talents and efforts of material scientists and structural engineers. As processing methods improve, the popularity of fabric-reinforced ceramic matrix composites will increase.

11.5 Time-Dependent Reliability

11.5.1 Introduction

The utilization of ceramic composites in fabricating structural components used in high temperature environments requires thoughtful consideration of fast fracture as well as strength degradation due to time-dependent

phenomena such as subcritical crack growth, creep rupture, and stress corrosion. In all cases, this can be accomplished by specifying an acceptable reliability level for a component. Methods of analysis exist that capture the variability in strength of ceramic composites as it relates to fast fracture (see Sections 11.2 through 11.4). However, the calculation of an expected lifetime of a ceramic component has been limited to a statistical analysis based on subcritical crack growth in monolithic materials (see Wiederhorn and Fuller[66] for a detailed development). The subcritical crack growth approach establishes relationships among reliability, stress, and time-to-failure based on principles of fracture mechanics. The analysis combines the Griffith[67] equation and an empirical crack velocity equation with the underlying assumption that steady growth of a preexisting flaw is the driving failure mechanism.

Several authors including Quinn,[68] Ritter *et al.*, [69] and Dalgleish *et al.*[70] have emphasized that time-dependent failure of monolithic ceramics is not limited to subcritical crack growth and may also occur by either stress corrosion or creep rupture. Stress corrosion involves nucleation and growth of flaws by environmental/oxidation attack. Creep rupture typically entails the nucleation, growth, and coalescence of voids dispersed along grain boundaries. The authors have similar expectations that these types of mechanisms will exist within the microstructure of ceramic composite constituents. However, the time-dependent mechanical response of a ceramic matrix composite will depend on how the material is loaded relative to the principal material direction. In this section, creep rupture is highlighted, and the intent is to outline a method that determines an allowable stress for a given component lifetime and reliability. One can assume that voids will nucleate, grow, and coalesce within the matrix first, and these voids will eventually produce a macrocrack within the composite, which is bridged by the fibers. Thus, one definition of component life is determined by the onset of the first transverse matrix crack. This is accomplished by combining Weibull analysis with the principles of continuum damage mechanics. Continuum damage mechanics was originally developed by Kachanov[71] to account for tertiary creep and creep fracture of ductile metal alloys. For this reason, many have wrongly assumed that the principles of continuum damage mechanics are only applicable to materials exhibiting ductile behavior. There are numerous articles (see, for example, Krajcinovic[72] and Cassenti[73]) that have advocated the use of continuum damage mechanics to model materials with brittle failure behavior.

Ideally, any theory that predicts the behavior of a material should incorporate parameters that are relevant to its microstructure (grain size, void spacing, etc.). However, this would require a determination of volume averaged effects of microstructural phenomena reflecting nucleation, growth, and coalescence of microdefects, that in many instances interact. This approach (see, for example, Ju[74]) is difficult, even under strongly simplifying assumptions. In this respect, Leckie[75] points out that the difference between the materials scientist and engineer is one of scale. He notes that the materials scientist is interested in mechanisms of deformation and failure at the

microstructural level, and the engineer focuses on these issues at the component level. Thus, the former designs the material and the latter designs the component. Here, the engineer's viewpoint is taken and it is noted from the outset that continuum damage mechanics does not focus attention on microstructural events, yet it does provide a practical model which macroscopically captures the changes induced by the evolution of voids and defects. As pointed out by Duffy and Gyekenyesi,[76] a comparison of the continuum and microstructural kinetic equations for monolithic ceramics yields strong resemblances to one another. Thus, the persistent opinion that phenomenological models have little in common with the underlying physics is sometimes short-sighted, and most times self-serving. Adopting a continuum theory of damage with its attendant phenomenological view would appear to be a logical first approach, and as Krajcinovic[77] notes, probably has the best chance of being utilized by the engineering community.

11.5.2 Damage State Variable

The evolution of the microdefects represents an irreversible thermodynamic process. At the continuum level, this requires the introduction of an internal state variable that serves as a measure of accumulated damage. Consider a uniaxial test specimen and let A_0 represent the cross-sectional area in an undamaged (or reference) state. Denote A as the current cross-sectional area in a damaged state where material defects exist in the cross-section (i.e., $A < A_0$). Microstructurally, this can be represented by Fig. 11.7. The macroscopic damage associated with this specimen is represented by the scalar

$$\omega = (A_0 - A)/A_0 \tag{47}$$

or alternatively by $\eta = 1 - \omega$, which is referred to as "continuity." This is the simplest manner in which to represent damage. The variable η represents the fraction of cross-sectional area not occupied by voids. A material is undamaged if $\omega = 0$ or $\eta = 1$. It is quite typical (and somewhat natural) to associate the thermodynamic state variable representing damage with a decrease in material integrity.

Note that, as it appears above, ω is a scalar quantity (i.e., a zero-order tensor). This is appropriate for the limited case where components are subjected to uniaxial loads and undergo isotropic damage. Here, isotropic damage is defined as a microstructure with microdefects that are randomly oriented and randomly distributed. A number of authors have alternatively treated the damage state variable as a vector (a first-order tensor), a second-order tensor, a fourth-order tensor, or an eighth-order tensor. Representing the damage state variable as a vector admits information relative to microcrack area and orientation, but anomalies arise in transforming this first-order tensor relative to a general multiaxial state of stress. Other authors have proposed using second-order tensors to model damage, but problems occur in representing anisotropic damage in general. Using fourth-order

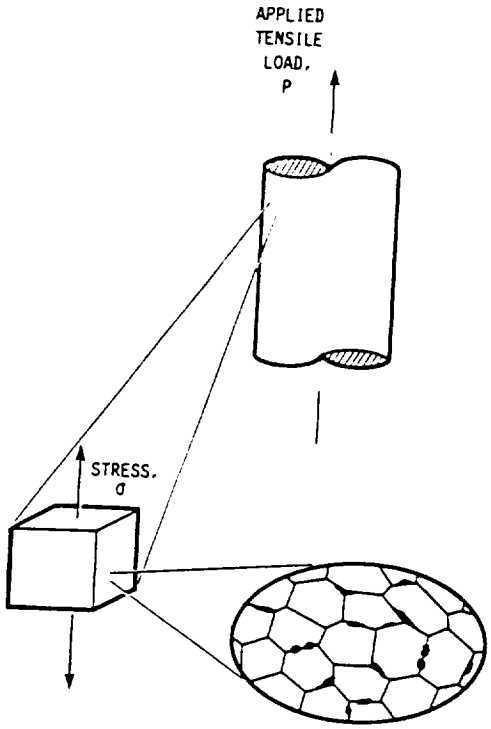

Fig. 11.7 Uniaxial tensile test specimen with distributed microdefects along the grain boundary.

tensors is appealing since an analogy can be made to the reduction (evolution) in stiffness properties that occurs in a damaged material. This analogy is illustrated using the concept of an effective stress.

The concept of an effective stress is based, in part, on the assumed existence of an elastic potential energy function that admits damage state variables. This function is a scalar valued function, and is defined by the expression

$$\Omega^e = (1/2)\,\eta\varepsilon_{ij}C^0_{ijkl}\varepsilon_{kl} \tag{48}$$

where C^0_{ijkl} is the undamaged (or reference) fourth-order elastic stiffness tensor, ε_{ij} is the second-order elastic strain tensor, and $\eta(=1-\omega)$ is initially taken as a scalar quantity to illustrate a deficiency associated with the scalar representation. Based on the assumed existence of Ω^e, and the Clausius–Duhem inequality, a homogenized stress tensor can be derived such that

$$\sigma_{ij} = \eta C^0_{ijkl}\varepsilon_{kl} \tag{49}$$

Thus, a damaged stiffness tensor can be easily obtained from Eqn. (49) and is given by the expression

$$C^d_{ijkl} = \eta C^0_{ijkl} \tag{50}$$

The result is that the elements of the damaged stiffness tensor are equal to the elements of the reference stiffness tensor reduced by a common factor η. This indicates that the amount of damage induced in a material can be quantified (or monitored experimentally) by the change in elastic stiffness properties. Note that these stiffness properties are macrovariables, and no assumption was imposed at this point regarding the original material symmetry (i.e., the undamaged material can be elastically isotropic or elastically anisotropic, the method admits either).

At this point, an effective stress can be defined by the expression

$$\bar{\sigma}_{ij} = \sigma_{ij}/\eta \tag{51}$$

Here, the principal orientations of the effective stress will coincide with principal orientations of the Cauchy stress (σ_{ij}) when the damage variable is a scalar. Through the use of an effective stress, the damage state variable can be incorporated directly into the Weibull equation (see Section 11.5.3). However, there are deficiencies in associating a scalar damage variable with a three-dimensional stress state. Specifically, Ju[74] has pointed out that a scalar damage variable will reduce the bulk and the shear moduli by an equal amount, that is

$$G^d = \eta G^0 \tag{52}$$

and

$$K^d = \eta K^0 \tag{53}$$

where G^d and K^d are damage shear and bulk moduli. This leads to

$$\frac{G^d}{K^d} = \frac{G^0}{K^0} \tag{54}$$

which implies that Poisson's ratio does not evolve (i.e., $\nu^d = \nu^0$). This is a rather strong restriction that has limited experimental support.[78] The physical implication of this is depicted in Fig. 11.8. Here, both the uniaxial stress–strain curve and the transverse strain are graphed. If the material damages in the load direction then the stress–strain curve changes slope. Even if the material damages isotropically, it would not seem reasonable that the transverse strain curve would be unaffected.

To circumvent this difficulty (and other difficulties associated with first- and second-rank damage tensors) it is more likely that a fourth-order tensor would better represent the damaged state of a material, whether the material is isotropic or anisotropic. Keep in mind that materials that are originally isotropic can damage in an anisotropic fashion. The result is an anisotropic

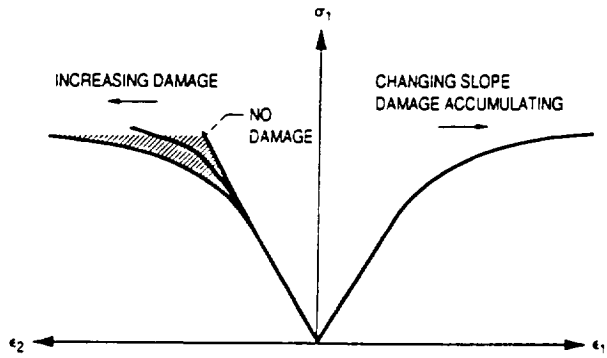

Fig. 11.8 Uniaxial stress–strain curve and possible transverse stress–strain curves for a material undergoing a damage process.

material. Once again, assuming the existence of an elastic potential energy function that admits a damage state variable, then

$$\Omega^e = (1/2)\,\varepsilon_{ij}\,\eta_{ijkl}(\omega_{mnop})\,C^0_{klrs}\,\varepsilon_{rs} \tag{55}$$

where $\eta_{ijkl}(\omega_{mnop})$ is a fourth-order tensor valued function that is dependent on a fourth-order damage state variable. Now, the Cauchy stress is given by the expression

$$\sigma_{ij} = \eta_{ijkl}(\omega_{mnop})\,C^0_{klrs}\,\varepsilon_{rs} \tag{56}$$

Thus, the effective stress and the Cauchy stress are related as follows

$$\sigma_{ij} = \eta_{ijrs}(\omega_{mnop})\,\bar{\sigma}_{rs} \tag{57}$$

where $\eta_{ijrs}(\omega_{mnop})$ is a transformation tensor. The simplest form of this transformation tensor is

$$\eta_{ijrs} = I_{ijrs} - \omega_{ijrs} \tag{58}$$

where I_{ijrs} is the fourth-order identity tensor. The effective stress tensor now becomes

$$\bar{\sigma}_{ij} = (I_{ijrs} - \omega_{ijrs})^{-1}\,\sigma_{rs} \tag{59}$$

where isotropic damage implies ω_{ijrs} is an isotropic fourth-order tensor, as opposed to stipulating that the damage state variable is a scalar which leads to unwarranted restrictions, as mentioned above. However, as long as uniaxial stress states are being considered it is not inappropriate to use a scalar damage state variable to illustrate how Weibull analysis can accommodate continuum damage mechanics to produce a time-dependent reliability model of practical utility. As a final comment, it would not be unreasonable to assume composite materials would undergo anisotropic damage, since these materials are anisotropic in the undamaged (or reference) state. Using a fourth-order tensor also allows modeling anisotropic damage in the most general fashion.

11.5.3 Damage Evolution

For time-dependent analysis, the rate of change of continuity $\dot{\eta}$ (or the damage rate $\dot{\omega}$) must be specified. This rate is functionally dependent on stress and the current state of continuity, that is

$$\dot{\eta} = \dot{\eta}(\sigma, \eta) \tag{60}$$

and is monotonically decreasing ($\dot{\eta} < 0$). For a uniaxial specimen, the dependence of $\dot{\eta}$ on stress is taken through a net stress defined as

$$\bar{\sigma} = P/A = \sigma_0/\eta \tag{61}$$

where P is the applied tensile load, and $\sigma_0 = P/A_0$. A power-law form of the kinetic equation is adopted, that is

$$\dot{\eta} = -B(\bar{\sigma})^n = -B(\sigma_0/\eta)^n \tag{62}$$

where $B > 0$ and $n \geq 1$ are material constants determined from creep rupture data, as discussed below. The authors recognize this form of evolutionary law is simplistic, stipulated *a priori*, and that experimental data may indicate some inconsistencies and/or inadequacies. Modification would be guided by experiment, and material science models for creep damage outlined in Duffy and Gyekenyesi.[76] As an example, physical processes that involve void growth mechanisms along grain boundaries typically exhibit threshold behavior. This is illustrated in a schematic plot of log of stress as a function of log of time-to-failure in Fig. 11.9. Marion *et al.*[79] suggest that along grain when stress levels are below a threshold value, liquid-phase sintered ceramics deform by a solution–precipitation mechanism without damage accumulation. Experimental data generated by Wiederhorn *et al.*[80] support the existence of this threshold for silicon nitride. Tsai and Raj[81] suggest methods of estimating values of a threshold stress for ceramics, and the above form of the kinetic equation could easily accommodate a threshold, that is

$$\dot{\eta}\begin{cases} = 0 & \sigma_0 \leq \sigma_{th} \\ = -B(\sigma_0/\eta)^n & \sigma_0 > \sigma_{th} \end{cases} \tag{63}$$

Dalgleish *et al.*[70] have presented experimental data that suggest the existence of a second threshold that delineates regions where subcritical crack growth and creep rupture failure mechanisms are operative. Chuang *et al.*[82] predict the value of this threshold stress by using principles of irreversible thermodynamics within the framework of several well-accepted models for crack growth. If this threshold (σ_{th}^*) exists, one can construct a composite reliability model such that

$$R\begin{cases} = R(\text{subcritical crack growth}) & \sigma_0 > \sigma_{th}^* \\ = R(\text{creep rupture}) & \sigma_{th} < \sigma_0 \leq \sigma_{th}^* \end{cases} \tag{64}$$

where R is the reliability of a component. Here, thresholds similar to those

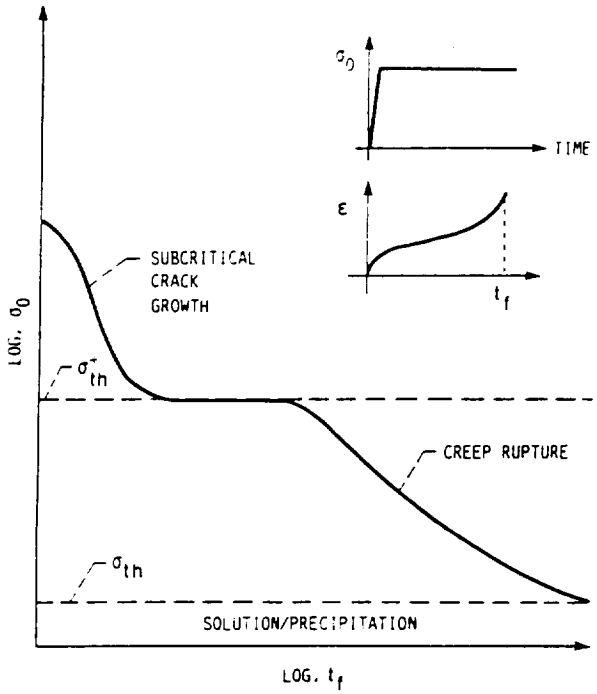

Fig. 11.9 Schematic plot of log of stress as a function of log of time to failure delineating threshold stresses, and outlining distinct regions where expected failure mechanisms would be operative.

outlined above for monolithic ceramics are recognized as a possibility for ceramic matrix composites. These thresholds would take on different values depending on the material orientation considered. However, a lack of quality experimental data leaves the authors unsure as to whether or not these thresholds are a universal phenomenon, and therefore ignoring the thresholds is expedient at this time.

It is postulated that during a creep rupture experiment σ_0 is abruptly applied and held at a fixed value (see the inset of Fig. 11.9). With $\eta = 1$ at $t = 0$, Eqn. (60) can be integrated to yield an expression for η as a function of time, stress, and model parameters, as follows:

$$\eta = [1 - B(\sigma_0)^n (n+1)t]^{1/(n+1)} \tag{65}$$

An expression for the time to failure (t_f) can be obtained from Eqn. (65) by noting that $t = t_f$ when $\eta = 0$. Hence

$$t_f = 1/B(\sigma_0)^n (n+1) \tag{66}$$

and the equation for η is simplified to

$$\eta = [1 - (t/t_f)]^{1/(n+1)} \tag{67}$$

This is consistent with the strong dependence of failure times on stress. However, the distribution of failure times for a given stress level σ_0 may be probabilistic or deterministic. Currently, the data are insufficient to postulate either case. Here, t_f is treated in a deterministic fashion noting that a probability distribution function for t_f could be introduced to the analysis in a manner similar to that suggested by Bolotin.[83]

To generate meaningful data, great care must be taken to determine the operative failure mechanism (i.e., subcritical crack growth or creep rupture). Dalgleish *et al.*[70] proposed using the Monkman–Grant constant to separate experimental rupture life data. However, the creep-damage tolerance parameter, defined by Leckie[84] as the total creep strain divided by the Monkman–Grant constant, may prove more suitable. After the data have been carefully screened, the model parameters n and B could be easily determined from creep rupture data. Taking the natural log of Eqn. (66) yields

$$\ln(t_f) + n\ln(\sigma_0) = -\ln[B(n+1)] \tag{68}$$

The value $1/n$ corresponds to the slope of $\ln(\sigma_0)$ plotted against $\ln(t_f)$, and B would be computed from the intercept.

11.5.4 A Reliability Theory Incorporating a Damage State Variable

Now consider that the uniaxial test specimen is fabricated from a ceramic material system with an inherent large scatter in strength. The variation in strength can be suitably characterized by the weakest link theory using Weibull's[85] statistical distribution function. Adopting Weibull's analysis, the reliability of a uniaxial specimen is given by the expression

$$R = \exp[-V(\sigma/\beta)^{\alpha}] \tag{69}$$

This assumes that the stress state is homogeneous and that the two-parameter Weibull distribution sufficiently characterizes the specimen in the failure probability range of interest. Taking σ equal to the net stress defined previously and, for simplicity, assuming a unit volume, yields the following expression for reliability

$$R = \exp[-(\sigma_0/\eta\beta)^{\alpha}] \tag{70}$$

Substituting for η by using Eqn. (65) gives

$$R = \exp\left\{-\left[\frac{\sigma_0}{[1 - B(\sigma_0)^n(n+1)t]^{1/(n+1)}\beta}\right]^{\alpha}\right\} \tag{71}$$

Alternatively, substituting for η by using Eqn. (67) yields

$$R = \exp\left\{-\left(\frac{\sigma_0}{\beta}\right)^{\alpha}\left[1 - \left(\frac{t}{t_f}\right)\right]^{-\alpha(n+1)}\right\} \tag{72}$$

Here, it is clearly evident that in the limit as t approaches t_f, R approaches zero. Examples of reliability curves and their dependence upon time and model parameters are presented and discussed in Duffy and Gyekenyesi.[76]

Next, the hazard rate function is considered. By definition, the hazard rate (or mortality rate) is the instantaneous probability of failure of a component in the time interval $(t, t + \Delta t)$, given that the component has survived to time t. In more general terms, this function yields the failure rate normalized to the number of components left in the surviving population. This function can be expressed in terms of R or the probability of failure P_f as

$$h(t) = -\frac{dR}{dt}\left(\frac{1}{R}\right) = \frac{dP_f}{dt}\left(\frac{1}{1-P_f}\right) \tag{73}$$

With Eqn. (72) used to define R, the hazard rate becomes

$$h(t) = \left(\frac{\alpha}{n+1}\right)\left(\frac{1}{t_f}\right)\left(\frac{\sigma_0}{\beta}\right)^{\alpha}\left[1-\left(\frac{t}{t_f}\right)\right]^{-(\alpha+n+1)/(n+1)} \tag{74}$$

The hazard rate function can be utilized from a modeling standpoint in one of two ways. First, it can be used graphically as a goodness-of-fit test. If any of the underlying assumptions or distributions used to construct Eqn. (72) are invalid, one would obtain a poor correlation between model prediction of the hazard rate and experimental data. On the other hand, experimental data can be used to construct the functional form of the hazard rate and R can be determined from Eqn. (73). In a sense, this latter approach represents an oversimplified curve-fitting technique. Since it was assumed that the creep rupture failure mechanism can be modeled by continuum damage mechanics, the first approach is adopted. In this spirit, the hazard rate function would be used to assess the accuracy of the model in comparison to experimental results.

As a final note, the relative magnitude of the hazard rate is interpreted as follows:

(1) A decreasing hazard rate indicates component failure has been caused by defective processing.
(2) A constant hazard rate indicates failure is caused by random factors.
(3) An increasing hazard rate denotes wear-out of the component.

Here, negative values of α and n are physically absurd, hence

$$-(\alpha+n+1)/(n+1) < 0 \tag{75}$$

and Eqn. (74) yields an increasing hazard rate. This is compatible with the underlying assumption that creep rupture is the operative failure mechanism if creep rupture is recognized as a wear-out mechanism.

11.6 Future Directions

Ceramic material systems will play a significant role in future elevated temperature applications. To this end, there are a number of issues that must be addressed by the structural mechanics research community. We begin by pointing out that recent progress in processing ceramic material systems has not been matched by mechanical testing efforts. There is a definite need for experiments that support the development of reliability models. Initially, this effort should include experiments that test the fundamental concepts embedded in the framework of current stochastic models. As an example, probing experiments could be conducted along various biaxial load paths to establish level surfaces of reliability in a particular two-dimensional stress space (similar to probing yield surfaces in metals). One could then verify such concepts as the maximum stress response which is often assumed in the multiaxial reliability models proposed for these materials. After establishing a theoretical framework, characterization tests would then be conducted to provide the functional dependence of model parameters with respect to temperature and environment. Finally, data from structural tests that are multiaxial in nature (and possibly nonisothermal) would be used to challenge the predictive capabilities of models through comparison to prototypical response data. These tests involve inhomogeneous fields of stress, deformation, and temperature, and would include two-bar tests as well as plate and shell structures. Results from structural testing provide feedback for subsequent modification. *Ad hoc* models result in the absence of structured interaction between the experimentalist and the theoretician. The validity of these models is then forever open to question. Furthermore, we cannot overemphasize that this genre of testing supports the development of methods for designing components, and not the material. Currently, this effort is hampered by the quality and scarcity of data. Ceramic properties pertinent to structural design, which include stochastic parameters, vary with test method. The mechanics research community is beginning to realize this, and a consensus is beginning to form regarding the adoption of standards. However, the authors wish to underscore the fundamental need for experimental programs that are relevant to structural mechanics issues.

The authors note that the discussion in previous sections for the most part focused on time-independent analyses. It should be apparent to the reader that the utilization of ceramics as structural components in harsh service environments requires thoughtful consideration of reliability degradation due to time-dependent phenomena. Mechanisms such as subcritical crack growth, creep rupture, and stress corrosion must be dealt with. Computational strategies are needed that extend current methods of analysis involving subcritical crack growth and creep rupture, to multiaxial states of stress. Furthermore, the bulk of current literature dealing with stress corrosion highlights experimental observations, with very little attention given to failure analysis. Several authors have suggested dealing with this mechanism analytically

through the use of chemical reaction rate theory. Indeed, this approach would be a good starting point, since it deals with the chemistry of failure at the microstructural level. In addition, if ceramic materials mimic ductile failure locally, cyclic fatigue will become a design issue. Under cyclic loads, the process zone advances as the crack tip extends and brittle fracture mechanics may need to be modified to account for pseudo-ductile fracture.[86] Hence, application of modified metallic fatigue analyses may be a distinct possibility. However, the development of current predictive methods for service life of ceramics is hampered by the lack of data (supporting the development of design protocols) on the behavior in various environments of interest.

Large strides have been made in understanding crack growth behavior in monolithic and whisker-toughened ceramics. However, one important aspect that has not been addressed in detail is the effect of rising R-curve behavior. Clearly, brittle materials need to be toughened, and this is often accomplished by creating a process zone around the crack tip. Within this zone, localized energy dissipation takes place which results in the development of increased damage tolerance through an increasing resistance to crack growth with crack extension. Under these conditions, fracture toughness becomes functionally dependent upon crack size. Failure of materials exhibiting rising R-curve behavior would not be dependent upon the initial distribution and orientation of flaw sizes, but on the rate at which resistance increases with crack growth. Several authors have discussed in theoretical terms the effect that R-curve behavior has on the stochastic parameters that are necessary for short-term failure as well as life prediction,[87] though again, very little data exist that correlate strength distribution to this behavior.

Current analytical research initiatives have focused on the analysis of first matrix cracking and ultimate strength (in the fiber direction) of an individual lamina. These analyses must be extended to multiple-ply failure in an angle-ply laminate. Failure in an individual ply causes local redistribution of the load to adjacent layers. In addition, delamination between laminae will relax the constraining effects among layers, which allows in-plane strains to vary in steps within a laminate. These effects require the development of rational load redistribution schemes. Failure analysis of woven ceramics must initially deal with quantifying damage induced by service loads in the absence of a discernible macrocrack. Furthermore, issues germane to component life, such as cyclic fatigue and creep behavior, must also be addressed analytically and experimentally.

Since ceramic composites, in general, and woven ceramic composites, in particular, have been identified by many government-supported technology demonstration projects (e.g., the EPM and HITEMP programs at NASA, the CFCC program at the DOE, and the IHPTET/NASP program sponsored by the Air Force) as high risk (but also high payoff) materials, industry has demonstrated a reluctance to invest the resources necessary to cover the research and development costs. For woven ceramic composites, current research efforts underway have been conducted at universities and in industry, but not

usually in conjunction with one another. Funded research at universities is mainly focused on composite mechanics to design the material, and in some cases on weaving technology needed to produce preforms. Industry is developing the high temperature processing technologies, which require substantial investments to bring this type of fabrication equipment on line. It strikes the authors that to minimize CMC product development cycles, more integrated efforts are needed that would develop transition to practice technologies such as structural analysis, testing, and nondestructive evaluation. This also points to the need for more concurrent engineering. Analysts may specify certain optimized architectures for strength, stiffness and toughness, but processing of these tailored composites may not be possible. Hence, designing components will require compromises between material scientists and design engineers. However, research in most CMC processing, testing and modeling is still in its infancy, especially when one compares them to the progress made in polymer matrix composites.

In closing, we recognize that when failure is less sensitive to imperfections in the material, stochastic methods may not be absolutely essential. Currently, imperfections can be found in abundance in ceramic matrix composites since the high processing temperatures required to fabricate components generate flaws and residual stresses as components cool down during fabrication. These materials exhibit a sensitivity to interface conditions, reaction among constituents, residual stresses, fiber bunching, misalignment, and also sensitivity to complex fiber architectures. However, a synergy effect is obtained since an individual matrix crack or fiber break will not cause macroscopic failure due to the structural redundancy of the microstructure. Trends in design protocols are moving in the direction of probabilistic analyses (even for metals) and away from the simplistic safety factor approach. In this sense, brittle ceramics will serve as prototypical materials in the study and development of reliability models that will act as the basis of future design codes.

References

1. B. W. Rosen, "Analysis of Material Properties," in *Engineered Materials Handbook Vol. 1—Composites*, ed. C. A. Dostal, ASM International, Materials Park, OH, 1987, pp. 185–205.
2. R. L. McCullough, "Micro-Models for Composite Materials—Particulate and Discontinuous Fiber Composites," in *Micromechanical Materials Modeling—Vol. 2*, eds. J. M. Whitney and R. L. McCullough, Technomic, Lancaster, PA, 1990, pp. 49–90.
3. F. F. Lange, "The Interaction of a Crack Front with a Second-Phase Dispersion," *Phil. Mag.*, **22**, 983–992 (1970).
4. A. G. Evans, "The Strength of Brittle Materials Containing Second Phase Dispersions," *Phil. Mag.*, **26**, 1327–1344 (1972).
5. D. J. Green, "Fracture Toughness Predictions for Crack Bowing in Brittle Particulate Composites," *J. Am. Ceram. Soc.*, **66**, C4–C5 (1983).
6. K. T. Faber and A. G. Evans, "Crack Deflection Processes—I. Theory," *Acta Metall.*, **31**[4], 565–576 (1983).

7. P. Angelini and P. F. Becher, "In Situ Fracture of Silicon Carbide Whisker Reinforced Alumina," *Ann. Meet. Electron Microsc.*, **45**, 148–149 (1987).
8. P. F. Becher, C. H. Hsueh, and P. Angelini, "Toughening Behavior in Whisker Reinforced Ceramic Matrix Composites," *J. Am. Ceram. Soc.*, **71**, 1050–1061 (1988).
9. R. C. Wetherhold, "Fracture Energy for Short Brittle Fiber/Brittle Matrix Composites with Three-Dimensional Fiber Orientation," *J. Eng. Gas Turbines Power*, **112**[4], 502–506 (1990).
10. S. B. Batdorf and J. G. Crose, "A Statistical Theory for the Fracture of Brittle Structures Subjected to Nonuniform Polyaxial Stresses," *J. Appl. Mech.*, **41**[2], 459–464 (1974).
11. T. T. Shih, "An Evaluation of the Probabilistic Approach to Brittle Design," *Engng. Fract. Mech.*, **13**, 257–271 (1980).
12. S. F. Duffy, J. M. Manderscheid, and J. L. Palko, "Analysis of Whisker-Toughened Ceramic Components—A Design Engineer's Viewpoint," *Ceram. Bull.*, **68**[12], 2078–2083 (1989).
13. S. F. Duffy and S. M. Arnold, "Noninteractive Macroscopic Statistical Failure Theory for Whisker Reinforced Ceramic Composites," *J. Comp. Mater.*, **24**[3], 293–308 (1990).
14. B. N. Cassenti, "Probabilistic Static Failure of Composite Material," *AIAA J.*, **22**, 103–110 (1984).
15. M. Reiner, "A Mathematical Theory of Dilatancy," *Amer. J. Math.*, **67**, 350–362 (1945).
16. R. S. Rivlin and G. F. Smith, "Orthogonal Integrity Basis for N Symmetric Matrices," in *Contributions to Mechanics*, ed. D. Abir, Pergamon Press, Oxford, 1969, pp. 121–141.
17. A. J. M. Spencer, "Theory of Invariants," in *Continuum Physics—Volume I*, ed. A. C. Eringen, Academic Press, New York, NY, 1971, pp. 239–255.
18. A. J. M. Spencer, "Constitutive Theory for Strongly Anisotropic Solids," in *Continuum Theory of the Mechanics of Fibre-Reinforced Composites*, ed. A. J. M. Spencer, Springer-Verlag, New York, NY, 1984, pp. 1–32.
19. R. C. Wetherhold, "Statistics of Fracture of Composite Materials," Ph.D. Dissertation, University of Delaware, Newark, DE, 1983.
20. S. F. Duffy and J. M. Manderscheid, "Noninteractive Macroscopic Reliability Model for Ceramic Matrix Composites with Orthotropic Material Symmetry," *J. Eng. Gas Turbines Power*, **112**[4], 507–511 (1990).
21. M. Miki, Y. Murotsu, T. Tanaka, and S. Shao, "Reliability of the Strength of Unidirectional Fibrous Composites," *AIAA J.*, **28**[11], 1980–1986 (1991).
22. P. de Roo and B. Paluch, "Application of a Multiaxial Probabilistic Failure Criterion to a Unidirectional Composite," in *Developments in the Science and Technology of Composite Materials*, eds. A. R. Bunsell, P. Lamicq, and A. Massiah, Association Européene des Materiaux Composites, Bordeaux, France, 1985, pp. 328–334.
23. K. J. Willam and E. P. Warnke, "Constitutive Models for the Triaxial Behavior of Concrete," *Int. Assoc. Bridge Struct. Eng. Proc.*, **19**, 1–30 (1975).
24. N. S. Ottosen, "A Failure Criterion for Concrete," *J. Engng. Mech.*, **103**[EM4], 527–535 (1977).
25. J. L. Palko, "An Interactive Reliability Model for Whisker-Toughened Ceramics," Masters Thesis, Cleveland State University, OH, 1992.
26. S. F. Duffy, A. Chulya, and J. P. Gyekenyesi, "Structural Design Methodologies for Ceramic Based Material Systems," in *Ceramics and Ceramic–Matrix Composites*, ed. S. R. Levine, ASME, New York, 1992, pp. 265–285.
27. C. T. Sun and S. E. Yamada, "Strength Distribution of a Unidirectional Fiber Composite," *J. Comp. Mater.*, **12**[2], 169–176 (1978).

28. K. Prewo and J. J. Brennan, "High-Strength Silicon Carbide Fiber-Reinforced Glass-Matrix Composites," *J. Mater. Sci.*, **15**[2], 463–468 (1980).
29. K. Prewo and J. J. Brennan, "Silicon Carbide-Yarn-Reinforced Glass-Matrix Composites," *J. Mater. Sci.*, **17**[4], 1201–1206 (1982).
30. J. J. Brennan and K. Prewo, "Silicon Carbide-Fiber-Reinforced Glass-Ceramic Matrix Composites Exhibiting High Strength and Toughness," *J. Mater. Sci.*, **17**[8], 2371–2383 (1982).
31. J. J. Blass and M. B. Ruggles, "Design Methodology Needs for Fiber-Reinforced Ceramic Heat Exchangers," ORNL/TM-11012, Oak Ridge National Laboratory, TN, 1990.
32. K. Friedrich, *Application of Fracture Mechanics to Composite Materials*, Elsevier Science Publishing Co., New York, NY, 1989.
33. B. Budiansky, J. W. Hutchinson, and A. G. Evans, "Matrix Fracture in Fiber-Reinforced Ceramics," *J. Mech. Phys. Solids*, **34**[2], 167–189 (1986).
34. D. B. Marshall, B. N. Cox, and A. G. Evans, "The Mechanics of Matrix Cracking in Brittle Matrix Fiber Composites," *Acta Metall.*, **33**[11], 2013–2021 (1985).
35. M. D. Thouless and A. G. Evans, "Effects of Pull-Out on the Mechanical Properties of Ceramic-Matrix Composites," *Acta Metall.*, **36**[3], 317–522 (1988).
36. M. Sutcu, "Weibull Statistics Applied to Fiber Failure in Ceramic Composites and Work of Fracture," *Acta Metall.*, **37**[2], 651–661 (1989).
37. H. E. Daniels, "The Statistical Theory of the Strength of Bundles of Threads," *Proc. Roy. Soc. Lond., Ser. A*, **183**[995], 405–435 (1945).
38. B. D. Coleman, "On the Strength of Classical Fibers and Fiber Bundles," *J. Mech. Phys. Solids*, **7**[1], 66–70 (1958).
39. B. W. Rosen, "Tensile Failure of Fibrous Composites," *AIAA J.*, **2**[11], 1985–1991 (1964).
40. C. Zweben, "Tensile Failure of Fiber Composites," *AIAA J.*, **6**[12], 2325–2331 (1968).
41. D. G. Harlow and S. L. Phoenix, "The Chain of Bundles Probability Model for the Strength of Fibrous Materials—I. Analysis and Conjectures," *J. Comp. Mater.*, **12**[2], 195–214 (1978).
42. S. B. Batdorf, "Tensile Strength of Unidirectionally Reinforced Composites—I," *J. Reinf. Plastics Comp.*, **1**[2], 153–164 (1982).
43. D. J. Thomas and R. C. Wetherhold, "Reliability Analysis of Continuous Fiber Composite Laminates," NASA CR-185265, National Aeronautics and Space Administration, Cleveland, OH, 1990.
44. H. F. Wu, "Statistical Analysis of Tensile Strength of ARALL Laminates," *J. Comp. Mater.*, **23**[10], 1065–1080 (1989).
45. T. G. Hu and D. B. Goetschel, "The Application of the Weibull Strength Theory to Advanced Composite Materials," in *Tomorrow's Materials: Today*, Vol. 1 (Proceedings of the 34th International SAMPE Symposium and Exhibition), eds. G. A. Zakrewski *et al.*, SAMPE, Covina, CA, 1989, pp. 585–599.
46. S. J. McKernan, "Anisotropic Tensile Probabilistic Failure Criterion for Composites," Masters Thesis, Naval Postgraduate School, 1990.
47. S. B. Batdorf and H. L. Heinisch, "Weakest Link Theory Reformulation for Arbitrary Fracture Criterion," *J. Am. Ceram. Soc.*, **61**, 355–358 (1978).
48. S. F. Duffy, J. L. Palko, and J. P. Gyekenyesi, "Structural Reliability Analysis of Laminated CMC Components," ASME 91-GT-210, Presented at the 36th International Gas Turbine and Aeroengine Congress and Exposition, Orlando, FL, 1991.

49. J. Margetson and N. R. Cooper, "Brittle Material Design using Three Parameter Weibull Distributions," in *Probabilistic Methods in the Mechanics of Solids and Structures*, eds. S. Eggwertz and N. C. Lind, Springer-Verlag, Berlin, Germany, 1984, pp. 253–262.
50. S. F. Duffy, L. M. Powers, and A. Starlinger, "Reliability Analysis of Structural Ceramic Components using a Three-Parameter Weibull Distribution," Paper presented at the 37th International Gas Turbine and Aeroengine Congress and Exposition, Cologne, Germany, 1992.
51. A. S. Fareed, M. J. Koczak, F. Ko, and G. Layden, "Fracture of SiC/LAS Ceramic Composites," in *Advances in Ceramics, Vol. 22: Fractography of Glasses and Ceramics*, eds. V. D. Frechette and J. R. Varner, American Ceramic Society, Westerville, OH, 1988, pp. 261–278.
52. F. Ko, M. Koczak, and G. Layden, "Structural Toughening of Glass Matrix Composites by 3-D Fiber Architecture," *Ceram. Eng. Sci. Proc.*, **8**, 822–831 (1987).
53. F. K. Ko, "Preform Fiber Architecture for Ceramic-Matrix Composites," *Ceram. Bull.*, **68**[2], 401–414 (1989).
54. T. W. Chou and J. M. Yang, "Structure-Performance Maps of Polymeric, Metal, and Ceramic Matrix Composites," *Metall. Trans.*, **17A**, 1547–1559 (1986).
55. T. W. Chou and T. Ishikawa, "Analysis and Modeling of Two-Dimensional Fabric Composites," in *Textile Structural Composites*, eds. T. W. Chou and F. K. Ko, Elsevier, New York, NY, 1989, pp. 209–264.
56. C. L. Ma, J. M. Yang, and T. W. Chou, "Elastic Stiffness of Three-Dimensional Braided Textile Structural Composites," in *Composite Materials: Testing and Design*, American Society for Testing and Materials, Philadelphia, PA, 1986, pp. 404–421.
57. J. M. Yang, C. L. Ma, and T. W. Chou, "Fiber Inclination Model of Three-Dimensional Textile Structural Composites," *J. Comp. Mater.*, **20**, 472–484 (1986).
58. F. K. Ko, C. M. Pastore, C. Lei, and D. W. Whyte, "A Fabric Geometry Model for 3-D Braid Reinforced Composites," Paper presented at Competitive Advances in Metals and Metals Processes, 1st International SAMPE Metals and Metals Processing Conference, Cherry Hill, NJ, August 1987.
59. R. M. Crane and E. T. Camponeschi, Jr., "Experimental and Analytical Characterization of Multidimensionally Braided Graphite/Epoxy Composites," *Exp. Mech.*, **26**[3], 259–266 (1986).
60. Z. G. Wang, C. Laird, Z. Hashin, W. Rosen, and C. F. Yen, "Mechanical Behaviour of a Cross-Weave Ceramic Matrix Composite," *J. Mater. Sci.*, **26**, 4751–4758 (1991).
61. A. Chulya, J. Z. Gyekenyesi, and J. P. Gyekenyesi, "Damage Mechanisms in Three-Dimensional Woven Ceramic Matrix Composites Under Tensile and Flexural Loading at Room and Elevated Temperatures," in *HITEMP Review 1991*, eds. H. Gray and C. Ginty, NASA CP-10082, National Aeronautics and Space Administration, Cleveland, OH, 1991, pp. 53.3–53.11.
62. C-F. Yen, Z. Hashin, C. Laird, B. W. Rosen, and Z. Wang, "Micromechanical Evaluation of Ceramic Matrix Composites," Final technical report submitted to Air Force Office of Scientific Research, Washington, DC, 1991.
63. N. K. Naik, P. S. Shembekar, and M. V. Hosur, "Failure Behavior of Woven Fabric Composites," *J. Comp. Tech. Res.*, **13**[1], 107–116 (1991).
64. J. M. Yang, "Modeling and Characterization of Two-Dimensional and Three-Dimensional Textile Structural Composites," Ph.D. Dissertation, University of Delaware, Newark, DE, 1986.

65. K. P. Walker, E. H. Jordan, and A. D. Freed, "Nonlinear Mesomechanics of Composites with Periodic Microstructure: First Report," NASA TM-102081, National Aeronautics and Space Administration, Cleveland, OH, 1989.
66. S. M. Wiederhorn and E. R. Fuller, "Structural Reliability of Ceramic Materials," *Mater. Sci. Eng.*, **71**, 169–186 (1985).
67. A. A. Griffith, "The Phenomena of Rupture and Flow in Solids," *Phil. Trans. Roy. Soc. Lond. Ser. A*, **221**, 163–198 (1921).
68. G. D. Quinn, "Delayed Failure of a Commercial Vitreous Bonded Alumina," *J. Mater. Sci.*, **22**, 2309–2318 (1987).
69. J. R. Ritter, Jr., S. M. Wiederhorn, N. J. Tighe, and E. R. Fuller, Jr., "Application of Fracture Mechanics in Assuring Against Fatigue Failure of Ceramic Components," NBSIR 80-2047, National Bureau of Standards, Washington, DC, 1980.
70. B. J. Dalgleish, E. B. Slamovich, and A. G. Evans, "Duality in the Creep Rupture of a Polycrystalline Alumina," *J. Am. Ceram. Soc.*, **68**, 575–581 (1985).
71. L. M. Kachanov, "Time of the Rupture Process Under Creep Conditions," *Izv. Akad. Nauk. SSR, Otd Tekh. Nauk*, **8**, 26 (1958).
72. D. Krajcinovic, "Distributed Damage Theory of Beams in Pure Bending," *J. Appl. Mech.*, **46**, 592–596 (1979).
73. B. N. Cassenti, "Time Dependent Probabilistic Failure of Coated Components," *AIAA J.*, **29**[1], 127–134 (1991).
74. J. W. Ju, "Damage Mechanics of Composite Materials: Constitutive Modeling and Computational Algorithms," Final technical report prepared for the Air Force Office of Scientific Research, Washington, DC, 1991.
75. F. A. Leckie, "Advances in Creep Mechanics," in *Creep in Structures*, eds. A. R. S. Ponter and D. R. Hayhurst, Springer-Verlag, Berlin, Germany, 1981, pp. 13–47.
76. S. F. Duffy and J. P. Gyekenyesi, "Time Dependent Reliability Model Incorporating Continuum Damage Mechanics for High-Temperature Ceramics," NASA TM-102046, National Aeronautics and Space Administration, Cleveland, OH, 1989.
77. D. Krajcinovic, "Damage Mechanics," *Mech. Mat.*, **8**, 117–197 (1989).
78. C. L. Chow and F. Yang, "On One-Parameter Description of Damage State for Brittle Material," *Engng. Frac. Mech.*, **40**[2], 335–343 (1991).
79. J. E. Marion, A. G. Evans, M. D. Drory, and D. R. Clarke, "High Temperature Failure Initiation in Liquid Phase Sintered Materials," *Acta Metall.*, **31**[10], 1445–1457 (1983).
80. S. M. Wiederhorn, D. E. Roberts, T.-J. Chuang, and L. Chuck, "Damage-Enhanced Creep in a Siliconized Silicon Carbide: Phenomenology," *J. Am. Ceram. Soc.*, **68**, 602–608 (1988).
81. R. L. Tsai and R. Raj, "Creep Fracture in Ceramics Containing Small Amounts of a Liquid Phase," *Acta Metall.*, **30**, 1043–1058 (1982).
82. T.-J. Chuang, R. E. Tressler, and E. J. Minford, "On the Static Fatigue Limit at Elevated Temperatures," *Mater. Sci. Eng.*, **82**, 187–195 (1986).
83. V. V. Bolotin, "Verification and Estimation of Stochastic Models of Fracture," in *Proceedings of the 1st USA-USSR Symposium on Fracture of Composite Materials*, Sijthoff and Noordhoff International Publishers, Alphen aan den Rijn, The Netherlands, 1979, pp. 45–54.
84. F. A. Leckie, "The Micro- and Macromechanics of Creep Rupture," *Engng. Frac. Mech.*, **25**, 505–521 (1986).
85. W. Weibull, "A Statistical Theory for the Strength of Materials," *Ingenoirs Vetenskaps Akadamien Handlinger No. 151*, The Royal Swedish Institute for Engineering Research, Stockholm, 1939.

86. R. O. Ritchie, "Mechanisms of Fatigue Crack Propagation in Metals, Ceramics and Composites: Role of Crack Tip Shielding," *Mater. Sci. Eng.*, **A103**, 15–28 (1988).
87. K. Kendall, N. McN. Alford, and J. D. Birchall, "Weibull Modulus of Toughened Ceramics," in *Advanced Structural Ceramics*, Vol. 78 (Materials Research Symposia Proceedings), eds. P. F. Becher, M. V. Swain, and S. Somiya, MRS, Pittsburgh, PA, 1987, pp. 189–197.